LENA DELTA WATER BODY MAPPING BASED ON RAPIDEYE SATELLITE IMAGE SERIES FOR DETERMINATION OF LAKE LEVEL HEIGHTS AND DELTA CHANNEL INCLINATION USING ALTIMETRY AND DEM DATA

Master thesis

M.Sc. Program for Polar and Marine Sciences POMOR

Saint Petersburg State University / Hamburg University

by

Aleksandr Volynetc

Saint Petersburg / Hamburg, 2017

Supervisors

Dr. F. Günther, Alfred Wegener Institute Helmholtz Centre for Polar and Marine Research, Potsdam, Germany

Dr. Fedorova I.V., Saint Petersburg State University, Institute of Earth Sciences, Saint Petersburg, Russia

Content

LENA DELTA WATER BODY MAPPING BASED ON RAPIDEYE SATELLITE IMAGE SERIES FOR DETERMINATION OF LAKE LEVEL HEIGHTS AND DELTA CHANNEL INCLINATION USING ALTIMETRY AND DEM DATA

Aleksandr Volynetc

Master Program for Polar and Marine Sciences POMOR / 022000 Ecology and environmental management

Supervisors:

Dr. F. Günther, Alfred Wegener Institute Helmholtz Centre for Polar and Marine Research, Potsdam, Germany

Dr. Fedorova I.V., Saint Petersburg State University, Institute of Earth Sciences, Saint Petersburg, Russia.

Past and present climate changes lead to a significant impact on dynamics of periglacial landscapes in Eastern Siberia. Thermokarst and polygonal lakes, ponds, watercourses and swamps are the inherent part of landscapes and primarily are subject to thermokarst and thermal erosion processes. The main objectives of master thesis are mapping of lakes and watercourses in the Lena Delta and adjacent Bykovsky Peninsula with subsequent determination of the height of the water's edge of these objects.

This region of interest is a notable as it is the largest arctic delta with its complicated geomorphological structure represented with three different in origin, structure and age main terraces. Such structure distinguishes the Lena Delta from other subarctic rivers deltas.

The study based on complex combination of Remote Sensing methods, GIS handling and statistical calculations. As initial data for the mapping of water bodies were used sets of high-resolution images acquired by two satellite surveying systems RapidEye and SENTINEL-2. To determine the height values of lakes was used TanDEM-X (TDX) digital elevation model. Received results were checked and compared with collected by GLAS laser altimetry data that was aboard ICESat satellite observing mission.

Statistical and visual analysis based on obtained map of lakes, watercourses of Lena delta with area more than 100 m² and Bykovsky Peninsula and the height of the water's edge of these objects allows differentiating terraces by limnicity and reflects differences in plane and altitude characteristics of lakes in different terraces. On the other hand, some generic features of the region were highlighted. Distribution of lakes and its areas by terraces demonstrated similarity with the results obtained in previous

studies. However using of high-resolution satellite imagery in this work allowed to take into account the influence of small lakes and consequently increased the detail of the map. Comparing the lake heights based on digital elevation model with averaged data of laser altimetry showed a correlation close to unity.

ОПРЕДЕЛЕНИЕ УРОВНЯ ОЗЕР И УКЛОНА ВОДОТОКОВ В ДЕЛЬТЕ РЕКИ ЛЕНЫ, ОСНОВАННОЕ НА МОЗАИКЕ КОСМИЧЕСКИХ СНИМКОВ, ДАННЫХ ЛАЗЕРНОЙ АЛЬТИМЕТРИИ И ЦМР

Волынец Александр

Магистерская программа «Полярные и морские исследования» («ПОМОР») / 022000 «Экология и природопользование»

Выпускная квалификационная работа магистра

Научные руководители:

Доктор Гюнтер Ф., Институт им. Альфреда Вегенера центр полярных и морских исследований им. Гельмгольца, Потсдам, Германия

Доцент, к.г.н. Федорова И.В., Санкт-Петербургский государственный университет, Институт Наук о Земле, Санкт-Петербург, Россия

Климатические изменения, как в прошлом, так и в настоящем, оказывают заметное влияние на динамику перигляциальных ландшафтов в Восточной Сибири. Термокарстовые и полигональные озера, водотоки и болота являются неотъемлемой частью таких ландшафтов и в первую очередь подвержены процессам термокарста и термоэрозии. Основными целями магистерской работы являются картографирование озер и водотоков в дельте Лены и на прилегающем к ней полуострове Быковский и последующее определение высоты уреза воды данных объектов.

Данная территория является примечательной в связи с тем, что представляет собой крупнейшую в арктическом регионе дельту, которая обладает сложной геоморфологической структурой, выраженной в трех различных по строению и возрасту главных террасах, что отличает ее от дельт других рек в субарктической зоне.

Проведенное исследование основано на комплексном сочетании методов дистанционного зондирования Земли (ДЗЗ), инструментария географических информационных систем (ГИС) и математической статистики. В качестве исходных данных для картографирования водных объектов использовались наборы снимков высокого разрешения спутниковых съемочных систем RapidEye, а также SENTINEL-2. Для определения высот озер использовалась цифровая модель рельефа (ЦМР) TanDEM-X (TDX). Для оценки точности полученных

высот в качестве эталона использовались данные лазерной альтиметрии GLAS, полученные со спутниковой системы ICESat.

Статистический и визуальный анализ, проведенный на основе полученной карты озер, водотоков дельты Лены площадью более 100 м² и полуострова Быковский, а также высот урезов воды озер, позволяет дифференцировать террасы по озерности и отражает различия плановых и высотных характеристик озер, расположенных на разных террасах. С другой стороны, были выделены некоторые общие черты распределения, соответствующие данному региону. Распределение озер и их площадей по террасам показало сходство с результатами, полученными в предыдущих исследованиях. Однако использование в данной работе спутниковых снимков высокого разрешения позволило учесть влияние небольших по площади озер и, как следствие, увеличило подробность карты. Сравнение высот озер, полученных на основе ЦМР с усредненными данными лазерной альтиметрии, показало корреляцию, близкую к единице.

1. Introduction

Current climate change is affecting arctic regions at a faster rate than the rest of the world. Over the last century the average surface temperature in the Arctic has increased by about 0.09 ºC per decade, a rate 50 % greater than that observed over the Northern Hemisphere as a whole (AMAP, 2011). A notably significant increase of air temperatures has been registered during the last decades and is projected to further rise. Such considerable changes potentially may have an impact on thaw-vulnerable permafrost landscapes, which occupy about 24% of the northern hemisphere's land mass (Zhang et al., 2008). Frozen ground contains a great amount of organic carbon, which can be released due to thawing of permafrost and accelerate climate warming (Grosse et al., 2011). For example, recent quantifications for the Holocene Lena Delta River terrace by Zubrzycki et al. (2013), which comprises the area of modern deltaic processes, mean soil organic carbon stocks for the upper 1 m of soils were estimated at 29 ± 10 kg m^{-2}.

Since natural systems and low-lying permafrost-dominated arctic river deltas in particular are sensitive to climate variability, climate change in polar region resulted in growing interest of geoscientists in Land-Ocean interactions including estuary dynamics and in close monitoring of the Arctic river deltas dynamics to better estimate landscape scale climate change impacts and to quantify carbon fluxes (Rachold et al., 2000; Are and Reimnitz, 2000; Grigoriev et al., 2004).

For several months in years 2016/2017 I conducted an internship in the Alfred Wegener Institute in the Periglacial Research Section in Potsdam (Germany). This section aims at the observation and quantification of current periglacial processes and environmental changes and their causes in order to assess the state of permafrost today and its future transformation (AWI, 2017). In order to better understand permafrost dynamics in far polar regions, remote sensing of landscape-scale changes is becoming an increasingly important method (Jorgenson and Grosse, 2016).

Permafrost, defined as the ground that remains at or below 0 ºC for more than two years and can be differentiated by its spatial extent into continuous (90–100%), discontinuous (50–90%), sporadic (10–50%), and isolated (0–10%) permafrost, as well as by its thickness, the amount of ground ice present, and its temperature (Grosse G. et al., 2013). Northeastern Siberia belongs to the zone of continuous permafrost. Arctic permafrost landscapes are among the most vulnerable and dynamic landscapes globally (Khury et al., 2013). One of the main destructive processes affecting permafrost is

thermokarst (Kokelj and Jorgenson, 2013). Thermokarst refers to the process by which characteristic landforms form following disturbance of the thermal equilibrium of the ground resulting in thaw of ice-rich permafrost or melting of massive ice (van Everdingen, 2005). Thermokarst is one of the most obvious types of permafrost degradation in arctic landscapes (Morgenstern et al., 2011). This process is usually expressed in formation, growth and vanishing of thermokarst lakes (Grosse et al., 2013) which are defined as lakes that usually occupy closed depressions formed by the settlement of frozen ground following thawing of ice-rich permafrost or melting of massive ice (van Everdingen, 2005). Thermokarst lakes and basins are ubiquitous landforms in ice-rich permafrost deposits in Siberia and typical features of the northern permafrost ecosystems. Thermokarst in East Siberian ice-rich permafrost massively developed at the transition from Pleistocene to Holocene, but after the Boreal period (9–7.5 ka BP), the thermokarst landscapes appeared as they do today and have experienced only minor changes since then (Morgenstern et al., 2013). Modern estimates of thermokarst lakes areal coverage span a wide range and are scale dependent, but obviously they can occupy a significant proportion of the land area in high latitude regions (up to 40% in some areas (Antonova et al, 2016). Therefore, it is obvious that arctic water bodies play a crucial role in land-atmosphere exchanges of greenhouses gases and energy fluxes. That is why the study of these objects is highly important for assessing the impacts global climate change on local (Boike et al., 2008; Muster et al., 2013).

Due to interaction between hydrosphere, lithosphere, atmosphere, biosphere and cryosphere arctic deltas are among the most dynamic and complex natural phenomena on earth (Walker, 1998). The Lena River Delta, situated in Northern Siberia, is one of key areas in these investigations because it is the largest delta in the Arctic. The importance of this place is also confirmed by long-term monitoring efforts at the research station on Samoylovskiy Island (Boike et al., 2013). Since natural deltas are characterised by complex geomorphological patterns, hydrological conditions and various types of ecosystems, precise and modern information on the distribution and extent of the delta water objects is necessary for a spatiotemporal assessment and accurate quantification of processes which drive the different types of changes in this region (Schneider et al., 2009)

Due to permafrost landscapes extent and remoteness, most of their changes remain unnoticed (Nitze and Grosse, 2016). Remote sensing techniques have the potential to afford precise and cost-effective means for observation, mapping and

analysis of Earth surface. These methods in geographical research provide a lot of opportunities and advantages especially for investigation of remote regions. Therefore these techniques are broadly applied for a large variety of 2D and 3D geomorpho-dynamic monitoring applications in the Laptev Sea region and the Lena Delta (Günther et al., 2013; Günther et al., 2015; Nitze and Grosse, 2016).

Lake level changes can be considered as one important indicator for the water balance in subarctic regions and for frozen ground mutability. Since the 1990s, satellite radar altimetry has effectively been used for monitoring the water surface elevation changes (Vu Hien Phan, Roderik Lindenbergh, 2011). However, although thermokarst lake change detection over time is a common remote sensing application (Kravstsova and Bystrova, 2009; Nitze et al., 2017), comprehensive inventories of thermkarst lakes with respect to lake water levels have been rarely carried out (Ulrich et al., 2017). It is worth saying that modern geographical studies are often based on GIS methods, which open a variety of opportunities for the processing initial data, analysis of spatial information and maps creation.

1.1. Objectives

The major objective of this work is to comprehensively map the spatial extent of water objects in the Lena Delta region at high resolution and to determine their water level height using remote sensing data and GIS methods. In order to realize this purpose, satellite images of the RapidEye and Sentinel-2 missions and the highly precise TanDEM-X digital elevation model (DEM) are used as input data.

Water level height of thermokarst lakes in the Lena Delta is an important indicator to assess the extent of permafrost degradation that this landscape has experienced in the past as well as to analyze the vulnerability of this region to future inundation against the background of current sea level rise, which has been observed to be around 1.84 mm per year in the Laptev Sea (Proshutinskiy et al., 2004). Moreover, thermokarst lake water levels may add to the existing knowledge of Lena Delta geomorphology (Grigoriev, 1993; Schwamborn et al. 2002) and reveal new insights into interesting spatial patterns of lake distribution. By this means, it is useful for a better understanding of arctic permafrost vulnerability against the background of climate warming influence on thermokarst processes.

Finally, this study is based on the theoretical and practical base in the research field of permafrost (i.e. French H. and Romanovskii N.), studies on thermokarst and thermokarst lakes (i.e. Fedorova I., Grosse G., Morgenstern A., Günther F., Shur Y.), and remote sensing (Grosse G., Günther F., Muster S.).

1.2. Study area

The Lena River Delta

The Lena River, which flows into the Arctic Ocean, is one of the biggest rivers in Russia: 4400 km long, the mean annual discharge rate is near 16 800 m^3/ s, the mean annual sediment flux is about 680 kg/s for suspended and 170 kg/s1 for bottom sediments according Alekseevsky, 2007. The months of maximal discharge is June one third of discharge occurs in this month (Walker, 1998). Thus the Lena river is the major terrestrial source of water and sediment for the Laptev Sea (Are & Reimnitz, 2000), and it forms the largest delta in the Arctic (Fedorova et al., 2015).

The delta (72.0–73.8° N, 122.0–129° E) is situated in North-Eastern Siberia and belongs to the typical Arctic tundra zone with continuous permafrost (Morgenstern et al. 2011). It is surrounded by the Laptev Sea to the west, north, and east and the Chekanovsky and Kharaulakh mountain ranges to the south (Nitze & Grosse, 2016).

The total area of the delta is over 2 000 km^2 and includes more than 1 500 islands of various size, about 60 000 lakes, and numerous branches of the Lena River (Are & Reimnitz, 2000). If the delta's upstream limit is set as including the Bulkurskaya Lena River branch to Tit-Ary Island, the delta area exceeds 32 000 km^2 (Fedorova et al., 2015). Schneider et al. (2009) obtained an area 29 036 km^2, which is 98% of territory. Thus according such estimation a total area of the Lena Delta equals 29630 km^2 (Bolshiyanov et al., 2013). According to Muster et al. (2012) 21 719 km^2 of this area represent land and the remaining areas are occupied by rivers and coastal zones.

One of the large islands in the delta, known as Erge-Muora-Sisse (Arga), has an area of 6997 km^2. The Lena River delta (fig. 1.1) is a complex of more than 800 arms with a total length of about 6 500 km. These branches flow in different directions, some of them diverging, others converging. There are four major branches in the delta. The main branch in the delta is the Trofimovskaya branch; from this branch the Sardakhskaya branch diverges after Sardakh Island. The second largest branch by volume is Bykovskaya channel that turns sharply to the east after Sardakh Island and

flows into Buor Khaya Gulf. The secondary branches are also Olenekskaya, which flows west into the Kuba Gulf, and the northward flowing Tumatskaya. Recently, a decrease in discharge has been observed in the Olenekskaya and Tumatskaya branches (Fedorova et al., 2015). Water bodies of different size, shapes, depths and types of formation cover about 20% of the delta's land area (Muster et al., 2012). A great number of ponds and lakes are presented in a variety of deltaic environments including old river channels, terrace-flank depressions, thaw depressions, inter- and intra-dune depressions, swales in ridges and swale deposits, low-centered polygons and the troughs between polygons (Walker, 1998). Most of these ponds are related to the permafrost.

The climate of the Lena River Delta area is characterized by extremely cold, long winters and short, cool summers. The annual mean air temperature on Samoylov Island from 1998–2011 was −12.5 ºC (Boike et al., 2013). During most of the year, the Lena Delta is in what might be called a "dormant state", in winter most of the water bodies are frozen to depths of 1.5 down to 3 m and ground water is immobilized (Walker, 1998).

Bykovsky Peninsula

The Bykovsky Peninsula and Khorogor Valley are part of the recent coastal lowland of the Laptev Sea and are situated in the Russian North-Eastern Siberia in southeastern direction of the Lena River Delta Grosse et al., (2005). An area of the Khorogor Valley is about 86.2 km² and an area of the BYK is about 172.5 km² (Grosse et al., 2005).

The peninsula is surrounded by large bays of the Laptev Sea. According to Grosse et al., (2007) the peninsula is an erosional remnant of a Late Pleistocene accumulation plain consisting predominantly of silty to sandy ice-rich permafrost deposits of the yedoma. Maximal elevation of this remnant on the Bykovsky Peninsula is about 43 m a.s.l., lower elevations of the Yedoma is about 25 m a.s.l. and of the peninsula 0 m a.s.l.

The permafrost in this region is continuous and reaches depths of 300–500 m. About 46% of the peninsula covered by deep thermokarst depressions (Grosse et al., 2005) appeared due to early Holocene climate warming (Grosse et al., 2008), the third part of thermokarst affected area is occupied by polygonal ponds and thermokarst lakes. Lakes, predominantly of early Holocene thermokarstic origin are abundant not only in the depressions, but also are situated on the yedoma uplands (Grosse et al., 2008).

Climate of the Bykovsky Peninsula is similar to the Lena Delta due to their close location.

1.3. Geomorphological and Geological settings

Three main geomorphological units (river terraces) in the Lena River Delta are identified by Schwamborn et al. (2002) after Grigoriev (1993) (fig. 1.1). The first terrace is characterized by ice-wedge polygonal tundra, large thermokarst lakes and active flood plains, which are affected by modern deltaic processes. This terrace formed during the Holocene and occupies most of the central and eastern parts of the delta. According to Schirrmeister et al., (2011), the second and third terraces, which dominate the western and partially southern parts of the delta, are erosional remnants of arctic paleolandscapes. The second terrace is characterized by frozen sediments that predominantly consist of fluvial sands, which are several tens of meters thick and that have been formed during the Late Pleistocene from > 52 to 16 kyr BP (Schirrmeister et al. (2011). This terrace features many large thermokarst lakes and is located in the northwestern part of the delta. The third and oldest terrace is an erosional remnant of a Late Pleistocene plain consisting of fine-grained, organic-rich and ice-rich sediments, characterized by polygonal ground and thermokarst processes (Schirrmeister et al., 2003). Continuous permafrost which is one of the most important factors in delta underlies the area to between about 400 and 600 m below surface (Grigoriev, 1960). It is represented here in form of ice wedges, which are expressed on the surface as ice-wedge polygons and pingos (Walker, 1998).

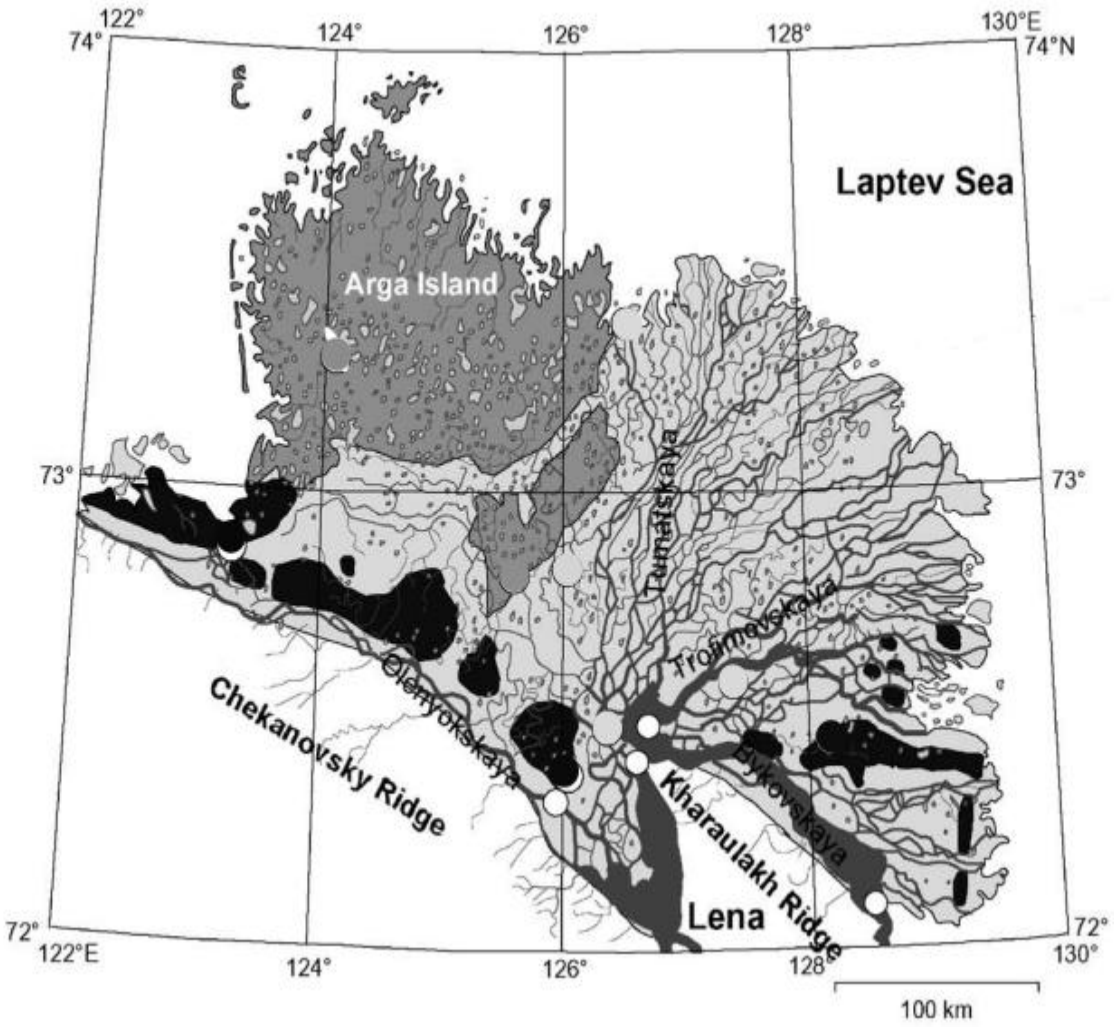

Figure 1.1. Geomorphological division of the Lena Delta (after Grigoriev, 1993; Schwamborn et al., 2002). Geomorphological units: black color – first terrace; grey – second terrace; light grey – first terrace. Circles – river bed sediments

An active role in the Lena Delta formation and evolution plays tectonism during the Pleistocene and also the Holocene. The modern seismicity indicates current vertical block movements. It was noted that Olenyokskaya and Bykovskaya channels flow in accordance with the general west-east direction of and along a Cenozoic fault line. Moreover, the Lena Delta can be divided into a structural eastern and a western part, which are charactzerised by general uplift and subsidence tendencies, respectively. This is believed to be caused by the continuation of the sub-longitudinal Gakkel Ridge, which crosses the Arctic Basin and propagates onto continental crust (Drachev et al., 1998). This suggestion proved not only through trough seismic data, but is also supported by geomorphological evidence such as a general drainage of most delta channels towards east. A key role in the area evolution played sedimentation of ice deposits during the Pleistocene that covered vast territories including most shallow shelf, and sea transgression during Holocene. The Lena River carries a huge volume of

suspended sediment. About 30 % of this load is thought to reach the Laptev Sea, while the remaining part of this volume is constantly redeposited between older islands, on sandbanks, or expands the delta towards the Laptev Sea (Fedorova et al., 2015).

Thus, the delta formed as a result of vertical tectonic movement, continuous sedimentation of Upper Pleistocene depositional units, on Holocene relief development, and modern hydrological processes of the Lena River. The pattern of the main channels is therefore predetermined by structural and near-surface geology, modern sedimentation, and hydrology

2. Materials and Methods

The main goals of this work is to map the spatial distribution of water bodies in the Lena Delta and to measure their water levels by means of remote sensing data and Geographical Information Systems (GIS) methods. To achieve these goals, the specific objectives are to:

- create a map of water objects in the delta;
- preprocess and correct DEM;
- combine the map of water objects with corrected DEM to retrieve lakes levels;
- process and statistically evaluate the obtained results.

The implementation of these plans demand a great amount of data and computer resources. The methodology and execution of this study is based on a combination of digital satellite image processing and GIS analyses.

Broad-scale processes in the Arctic, such as hydrological, vegetation or climate dynamics, are generally monitored with remote sensing data at different temporal and spatial resolutions, but most often with resolution of 250 m or coarser (Stow et al., 2004; Beck & Goetz, 2011; Fensholt & Proud, 2012; Goetz et al., 2011; Urban et al., 2014). However, this scale is usually not sufficient enough to study different natural processes in the Arctic such as thermokarst. Therefore, a large variety of remote sensing studies employing higher resolution satellite imagery in conjunction with data obtained during field expeditions have already been conducted in the past (i.e. Ulrich et al., 2009, Morgenstern et al., 2011, Muster et al., 2012, Günther et al., 2015). Due to spatial limitations of the remote sensing data that has been used in all these studies (i.e. ALOS, Chris Proba, and airborne photography), only selected field sites have been analyzed at a higher level of detail. In contrast Schneider et al. (2009) and Nitze and Grosse (2016) used Landsat data with 30 m pixel size in order to characterize land cover classes and land surface changes. Concerning the high heterogeneity of tundra surfaces in the region of interest (the Lena Delta), it is important to take into consideration the effect of mixed pixels, since many river distributaries, islands, lakes, and ponds are relatively small. Therefore, it is of great value to use higher resolution remote sensing data, in order to more precisely discriminate distinct features, such as water bodies for further study.

2.1. Data

2.1.1. Satellite images

For creation of a Lena Delta water-objects database, 58 high-resolution (ground sampling distance: 6,5 m) multi-temporal RapidEye satellite images were acquired within the framework of the RapidEye science archive (RESA) special area project "Remote sensing of permafrost thaw-related landscape dynamics in the Lena Delta region: coastal erosion, river delta changes, and thermokarst" (principal investigator Frank Günther) (fig. 2.1). The images were provided at processing level 1B and span a time period from June 2009 to September 2015 (tab. 2.1). The RapidEye images which cover almost entire Lena Delta provide 5 spectral bands:

1. Blue (440-510 nm);
2. Green (520–590 nm);
3. Red (630–685 nm);
4. Red Edge (690–730 nm);
5. Near infrared (NIR) (760–850 nm).

RapidEye – is the commercial operational class Earth observation system using a constellation of 5 satellites that provide unparalleled performance in order to achieve a high revisit frequency and thus temporal resolution, which can be used for change detection purposes and to capture seasonal variability (Behling et al. 2014),.

The RapidEye Basic product is radiometric and sensor corrected, providing imagery from the spacecraft without correction for any geometric distortions inherent in the imaging process. Prior to direct georeferencing, the spectral characteristics of all 56 images have been normalized by atmospheric correction (ATCOR module of PCI Geomatica) to top of atmosphere reflectance at particular dates and under consideration of varying solar zenith and solar azimuth values, and subarctic summer rural conditions. Although the imagery is not mapped to a cartographic projection, the wide area imagery (70 x 140 km) comes with rational polynomial coefficients (RPC) that provide all spacecraft telemetry for geometric processing of the data into a geo-corrected form. Based on orthorectified (terrain corrected) very high resolution (0.5 m pixel size) GeoEye and WorldView satellite images that were available for three key regions (Kurungnakh, Sobo-Sise, and Bykovsky Peninsula) distributed across the southern Lena Delta, ground control points were collected for RapidEye scenes overlapping with these sub regions. Finally, based on RPCs, all remaining RapidEye scenes have been included

into the bundle block adjustment procedure through a large amount of common points (tie points) between images that were collected automatically. By this means, handling of all images within one adjustment procedure not only provides a highly self consistent set of satellite images relative to each other, but also in absolute geocoding accuracy. Finally, the atmospherically corrected images were orthorectified based on DEM terrain elevation data and resampled to 5 m spatial resolution within the UTM 52N coordinate system.

The Provided images represent different years and different seasons, because images for one year or one season don't cover all parts of the Lena Delta due to frequent cloud cover. Although this seems to be not ideal from a perspective of capturing equal conditions, it offers the possibility to actually map the entire delta with all its strong seasonal variations from snow melt water saturated surfaces to dry conditions in late summer and phenological vegetation cover changes.

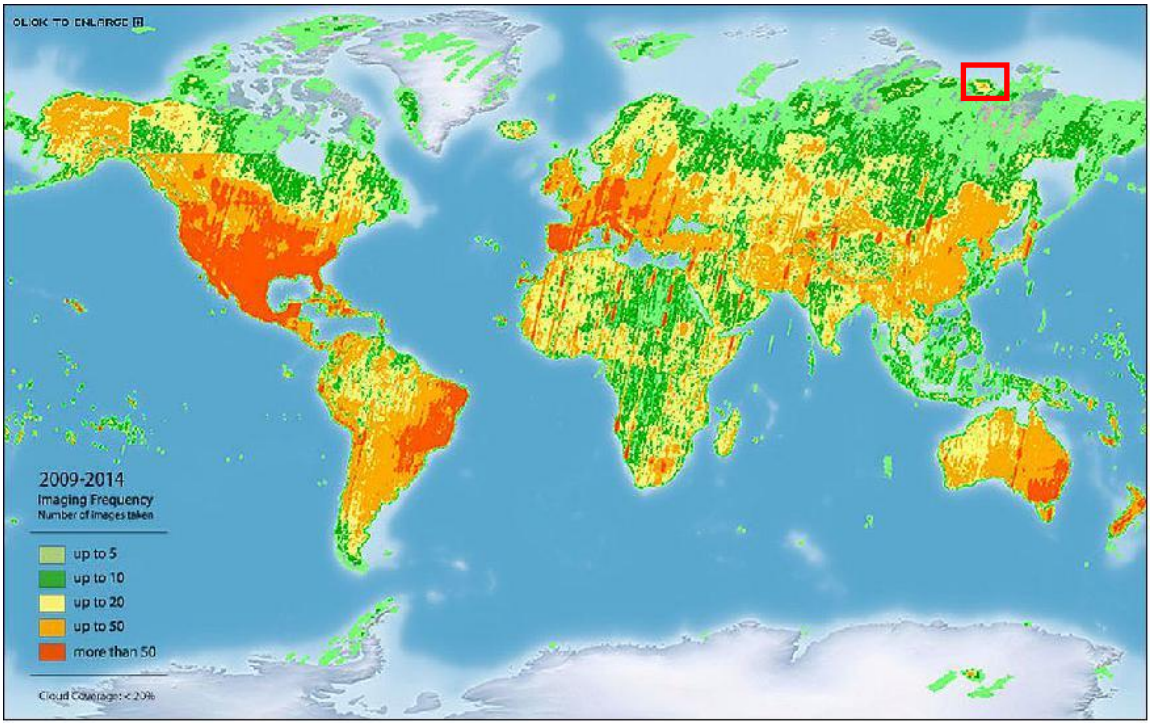

Figure 2.1. Imaging frequency of the RapidEye archive data between the start of operations in February 2009 to June 30, 2014 (eoportal.org), red frame outlines the extent of the Lena Delta special area RapidEye Science Archive project

With respect to these effects, a review of obtained RapidEye data showed that only images acquired during late spring, summer and early September can be further considered to get a correct result. Because during the second half of autumn winter and spring the territory is covered by snow and water bodies are covered by ice. Therefore,

after whole data preprocessing path only 46 georeferenced and orthorectified images, that present late June to early September conditions were used in a further analyses (tab. 2.1).

Table 2.1. Data acquisition

year	months	Number of shots
2009	June, July	5
2010	July, August	8
2011	June, July, August	5
2014	May, June, July, August, September	19
2015	June, July, August, September	9
2016	September	5 (SENTINEL-2 images)

Although a lot of RapidEye images were acquired, still some data gaps in the southwestern and northwestern part of the delta remained. In order to fill these gaps it was decided to use also SENTINEL-2 images. Since five Sentinel-2 images acquired in September 2016 covered the entire region of our interest, they have been used not only to fill the data gaps, but also as another independent dataset for water body mapping across the entire delta. Thus was chosen 5 images for September 2016 with channels Resolution of 10 meters.

SENTINEL-2 is a European wide-swath, high-, pushbroom multi-spectral imaging. The full mission specification of the twin satellites flying in the same orbit but phased at 180°, is designed to give a high revisit frequency in 13 bands with different spatial resolution (Sentinel-2_User_Handbook).

Within this project, 5 SENTINEL-2 images, each containing 4 Visible-Near Infrared (VNIR) bands (490 nm (B2), 560 nm (B3), 665 nm (B4), 842 nm (B8) with a resolution of 10 meters were used. Similar to the RapidEye data, all SENTINEL-2 images have been atmospherically corrected and radiometrically normalized. Because of the higher spatial resolution of the RapidEye imagery, SENTINEL-2 images were then slightly adjusted to this dataset by using only common feature tie-points. Due to near nadir viewing geometry of SENTINEL-2 and given the generally flat topography in the study region, no additional orthorectification was carried out.

2.1.2. Digital Elevation Model

As the base for elevation measurements the TanDEM-X DEM was used. TanDEM-X DEM is global Digital Elevation Model (DEM) of the land masses of the Earth. This DEM was generated from bistatic X-Band interferometric SAR acquisitions from two satellites (TerraSAR-X (TSX) and a second satellite TanDEM-X (TDX), which orbit Earth at an altitude of around 500 kilometers (EOC TanDEM-X, 2016). TanDEM-X DEM data is provided at either 12 m or 30 m nominal ground resolution. Here the higher elevation product is used, which has been granted to AWI based on the DEM_GEOL_1684 proposal "Application of TanDEM-X elevation data for remote sensing change detection of permafrost thaw in the Laptev Sea region" (Principal investigator Frank Günther).

The elevations are defined with respect to the reflective surface of X-Band interferometric SAR returns. Therefore, the TanDEM-X DEM products represent predominantly a Digital Surface Model (DSM), which generally corresponds to ground elevation in this tundra environment. The acquisition of this model took four years, from December 2010 to January 2015. In order to reach the target accuracies all land masses are covered at least twice in the same looking direction, but with different baselines (EOC TanDEM, 2016).

The elevation values of the initial DEM sub-tiles represent the ellipsoidal heights relative to the WGS84 ellipsoid in the WGS84-G1150 datum. One elevation value h reflects a weighted height average for a given pixel, computed by the height values of all contributing DEM scenes (EOC TanDEM-X, 2016). Extreme important parameters which determine the quality and applicability of each DEM are different types of accuracy:

1. Absolute horizontal accuracy is defined as the uncertainty in the horizontal position of a pixel with respect to a reference datum, caused by random1 and uncorrected systematic 2 errors. The value is expressed as a circular error at 90% confidence level.
2. Absolute vertical accuracy is the uncertainty in the height of a pixel with respect to a reference height caused by random and uncorrected systematic errors. The value is expressed as a linear error at 90% confidence level.
3. Relative vertical accuracy is specified in terms of the uncertainty in height between two points (DEM pixels) caused by random errors. The corresponding values are expressed as linear errors at 90% confidence level (LE90) [A1]. The reference area for two height estimates is a 1° x 1° area, corresponding to approximately 111 km x 111 km at the equator.

The spatial resolution is determined by the pixel spacing in latitude direction is 0.4 arcseconds, which corresponds to 12.37 meters at the equator and to 12.33 meters near the poles and in longitudinal direction in zone between 70° – 80° North/South it equals to 1.2'' (12.69m – 6.44m) (EOC TanDEM-X, 2016)

Table 2. 2. Specification of accuracy of the TanDEM-X DEM (2016).

DEM Product	Independent Pixel Spacing	Absolute Horizontal Accuracy, CE90	Absolute Vertical Accuracy, LE90	Relative Vertical Accuracy, 90% linear point-to-point error	Coverage
TanDEM-X DEM					
TanDEM-X DEM **(standard product 0.4 arcsec)**	**~12 m** **(0.4 arcsec @ equator)** see Sec. 4.3.1.3	**<10 m**	**<10 m**	**2 m (slope ≤ 20%)** **4 m (slope > 20%)**	**global**

For the Lena Delta region one product tile has an extent of 1° x 2°. It means that to cover the entire region it was necessary create a mosaic of nine TanDEM-X tiles that was done using GEOMATICA software. Tandem mosaic was reprojected from the initial Geographical Coordinate System on the ellipsoid WGS84-G1150 to the geodetic coordinate system UTM WGS84 52N which is suitable for the Lena Delta. In order to consider geoid height undulations, it was decided to transform ellipsoidal elevation values to heights above mean sea level (m a.s.l), therefore the values of DEM were recalculated from elevations above ellipsoid WGS84-G1150 to m a.s.l. heights using the geoid EGM2008 at 2.5' spacing.

2.1.3. Additional GIS layers

In this work polygon vector layers containing the spatial extent of terraces in the Lena Delta were provided as ready to use dataset by Anne Morgenstern, see Morgenstern et al. (2008, 2011).

Space-borne laser altimetry data (Release 34) from the Geoscience Laser Altimeter System (GLAS) instrument that was aboard the NASA Ice, Cloud, and land Elevation (ICESat) satellite has been obtained from the National Snow & Ice Data Center (NSIDC) in Boulder (USA). The data were processed by Frank Günther for the study region considering only measurements with laser transmit energies below 30 millijoules, in order to exclude possible cloud height measurements. A correction to

elevation for saturated waveforms has been applied. Since ICESat uses another ellipsoid (Topex/Poseidon) elevation values had to be converted to WGS84 ellipsoidal heights and finally to heights in m a.s.l. for comparison with TanDEM-X data. ICESat acquired data during several single campaigns between February 2003 and October 2009. Point measurements of the earth surface elevation within 35 m radius footprints had a 175 m spacing along-track and 16 – 25 km across track in the Lena Delta (fig. 2.2).

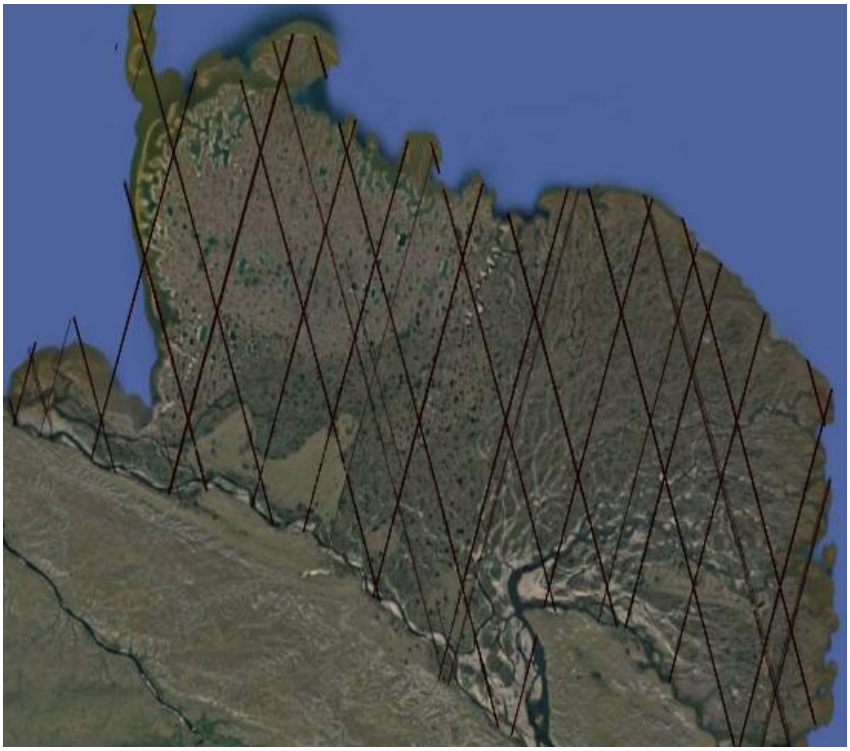

Figure 2.2. Image map (Google Maps) over the Lena Delta with ICESat/GLAS tracks

2.2. Methods

2.2.1. Satellite images sets processing

In order to receive a consistent scheme of water objects with elevations we applied a strategy of data refinement, fusion, examination and analysis to the study area. Accurate mapping and heights determination using multi-temporal, multi-platform remotely sensed data requires consideration of various distortions, including distortions associated with the platform, the map projection, and shape of the earth's surface (Gunther et al., 2013). For the overview and preprocessing (fig. 2.3.) of satellite images was used Geomatica software package provided by PCI Geomatics.

Optical remotely sensed data are expressed in arbitrary units such as digital number (DN), and always affected by sensor characteristics, illumination geometry and atmospheric conditions (Vaudoura et al., 2014). The atmospheric effects influence on the signal registered by remote sensors should be minimized using special methods in order to provide reliable spectral information (Bernardo et al., 2017). Atmospheric correction allows researchers eliminate different types of clouds, hazes and convert digital numbers into relatively similar surface reflectance taking into account various factors.

PCI Geomatica‘s Atmospheric Correction provides a variety of atmospheric corrections methods (PCI, 2015).

From several techniques for atmospheric correction was chosen ATCOR - Ground Reflectance workflow, which calculates ground reflectance values for supported optical imagery and optionally performs haze removal and cloud masking (fig. 2.3). The output is in reflectance values (0 - 100%), which are based on processed digital numbers (PCI, 2015).

Geomatica software package allows automatize an algorithm of processing by means of model creating for batch processing of remotely sensed data. The modeller module provides access to a number of standard operations such as data import and export, as well as most PCI Geomatics processing algorithms (PCI, 2015). This opportunity was used for automatization of further data pre-processing steps, such as atmospheric correction.

For this correction, a model was created, which uses all the metadata of the ingested imagery, terrain elevation information (DEM), which was provided by AWI Potsdam and visibility information/settings (Atmospheric conditions – Subarctic Summer, Aerosol type - Rural, visibility – 100 km.). All images were corrected this way.

The whole set of RapidEye and SENTINEL-2 images covers an area wider than the actual Lena Delta. Consequently, in order to accelerate the data processing it was necessary to exclude areas which don’t correspond to our region of interest from all images by creating appropriate clip masks.

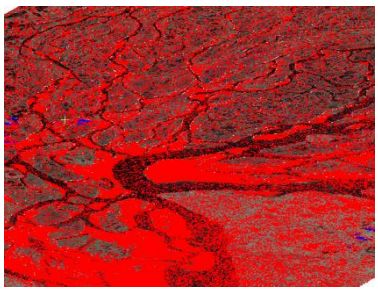

Figure 2.3. Result of haze and cloud masking. Blue spots – cloud mask, red spots – haze mask

Before the remotely sensed information can be gathered in a manner that is suitable for a mapping or GIS analysis, the imagery data must be prepared in a way that corrects different distortion effects and transforms in the required projection. Transfer of satellite image to the geometry of the map consists of georeferencing - correction for distortions connected with the acquisition system, transformation in the required projection (gis-lab.info, 2012); and orthorectification correction for relief-induced displacement effects using a rigorous math model and a digital elevation model (F. Günther et al.: The disappearing East Siberian Arctic island Muostakh). To carry out computation of the math model and orthorectification Geomatica's module OrthoEngine was used (fig. 2.4).

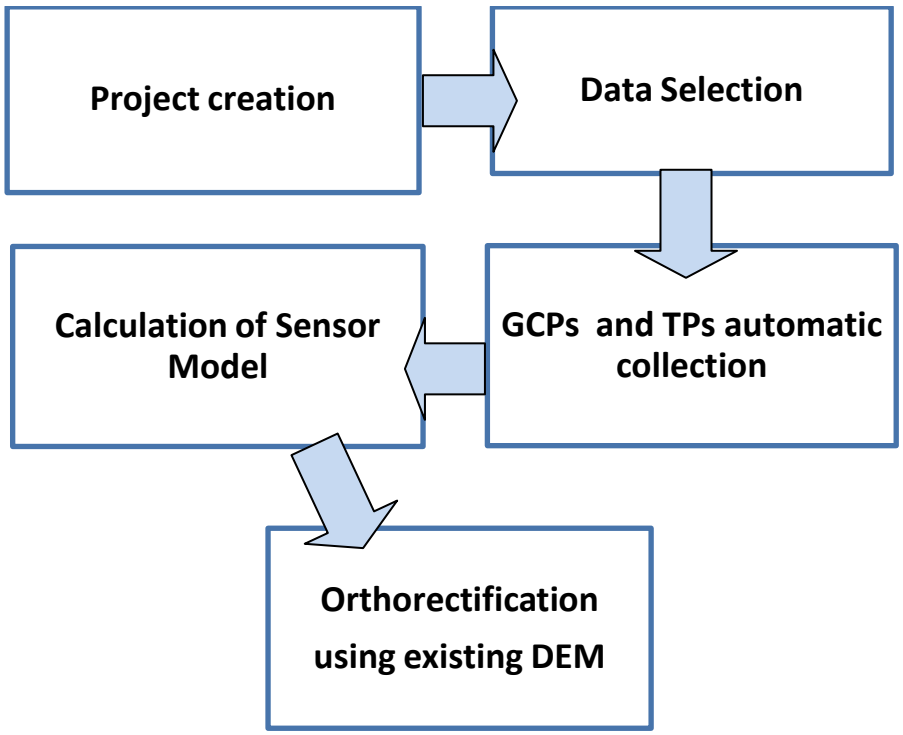

Figure 2.4. Satellite orbital modeling workflow diagram

Processing of RapidEye imagery was done within an OrthoEngine project with Math Modelling Method for optical satellite data based on Rational Functions Math

Model. The Rational Functions Math Model is a simple Math Model that builds a correlation between the pixels and the ground locations. The math model is computed for each image separately using four polynomials, which are functions of latitude, longitude, and height or elevation. To obtain polynomial coefficients it is necessary to collect Ground Control points. A ground control point (GCP) is feature that can be clearly identified in the raw image for which ground coordinates there are known and determines the relationship between the raw image and the ground by associating the pixel and line image coordinates to the x, y, and z coordinates on the ground (PCI, 2015).

Although the western part of the Lena Delta belongs to UTM 51N zone, the project coordinates were WGS 84 UTM projection Zone 52N, because all of the reference data for ground control point collection were located in the eastern part of the Lena Delta. Ground control points were sampled automatically from already rectified and georeferenced (geocoded) 4 GeoEye images with ultrahigh resolution, which were provided by AWI Potsdam. Expanding manual ground control point collection with automatic collection, it has been possible to exclude inaccurate points and to constantly correct the image model during iterative refinements based also on tie points. Manual correction mostly comprised removal of false points with unacceptable errors, often situated on the water or clouds.

As a result 271 ground control points were obtained. It should be noted that there was a lack of ground control points for the western part of Lena Delta, because all rectified GeoEye images are situated in the Eastern part of the Lena Delta, which could have an influence on the accuracy of the rectification. 30 Ground Control points with significant residual errors were transferred to Check Points to get the independent accuracy assessment of the math model, because check points aren’t considered during math model calculation.

In order to extend ground control over entire area and therefore beyond the ground control clusters, 7013 tie points were collected automatically for 58 images. A tie point is a feature that is clearly identified in two or more images and that can be selected as a reference point. These points identify how the images in the project relate to each other. The result of sampling was corrected manually. Using collected Ground Control Points and Tie Points a rigorous math model was computed for 55 images that is often referred to as a bundle adjustment. The math-model solution calculates the position and orientation of the sensor—the aerial camera or satellite—at the time when

the image was taken, GCPs, wherein tie points are automatically weighted inversely to their estimated errors (PCI, 2015).

For project quality estimation in addition to Check Points, Root Mean Squared (RMS) Errors for the entire project were calculated on the base of single image Residual Errors. Residual Error is the difference between the real coordinates of the ground control points or tie points and where those points are according to the computed math model (PCI, 2015). As a rule of thumb, a reasonable RMS error generally should be around half of the resolution of the image (one pixel), in case of this project, it means that residual errors should be under 6.5 meters.

Table 2.3. Residual Summary for 55 Images

	number	X RMS	Y RMS
GCPs	271	0.28	0.32
Check points	30	0.85	0.83
Tie points	7013	0.13	0.15
RMS (x,y,z) for worst 5% of points 0.66, 0.74			

The final Math Model and the Digital Elevation Model were used for orthorectification of RapidEye images. Resampling of pixels (extraction and interpolation of the grey levels from the original pixel locations to the corrected locations) were carried out using Cubic convolution method, which determines the gray level from the weighted average of the 16 closest pixels to the specified input coordinates and assigns that value to the output coordinates. The resulting image is slightly sharper than one produced by Bilinear Interpolation, and it does not have the disjointed appearance produced by Nearest Neighbor Interpolation (PCI, 2015).

Actually SENTINEL – 2 images are already snapped with the precision higher than 1 pixel but because of discovered difference in spatial position between SENTINEL – 2 and RapidEye images, SENTINEL-2 imagery was also decided to georeference in Geomatica OrthoEngine using RapidEye dataset.

To map water objects two different methods were tested:

Firstly it was tried to create mosaic of RapidEye image for the whole Lena Delta and then classify it using combination of Unsupervised and Supervised image classification in PCI Geomatica. Obtained results were unsatisfactory due to several classification problems that mostly were related to strong seasonal variability of the lake water turbidity. While many lakes showed very clear water conditions, others nearby exhibit very turbid sediment loaded water surfaces that were misclassified as land. This

couldn’t be solved with additional and refined training areas because of the limited spectral information with five bands.

The second method, which is finally used in this study imply the extraction of water objects from every single image using only the NIR channel. This approach requires following preprocessing steps: NIR channels extraction – images in NIR channel correction (clipping of regions with cloud shadows). After considering seasonal aspects and image coverage inspections, 35 RapidEye and 5 SENTINEL-2 images were used for further water body mapping.

2.2.2. Creation of water mask

The extraction of water objects was based on an empirical threshold that has been determined in top of atmosphere reflectance RapidEye and SENTINEL-2 images. Because of varying spectral band characteristics between RapidEye and SENTINEL-2, mapping was done separately for each of both datasets, but followed a common approach:

1. Overlay of all images and searching for the minimum value at a particular pixel location, where then each output cell value is a minimum value of the values assigned to the corresponding cells in the input raster map layers using algorithm GRASS r.series (grass.osgeo, 2017). (fig. 2.5a)
2. As pixel value domain which has been determined as being associated with open water, two separate ranges from 0.1 to 8.8 and from 0.1 to 2.7 for RapidEye and SENTINEL-2, respectively were used. This separate treatment has been necessary, because after atmospheric correction with the same settings, images from these two systems showed different incomparable reflectance values. This selection was also done using GRASS r.series (grass.osgeo, 2017). As a result, two different layers portraying water bodies of the Lena Delta were obtained (fig. 2.5 b, c).
3. Received rasters were converted into binary form using GDAL raster calculator (fig. 2.6 a, b).
4. Obtained rasters contained noise (a lot of small objects and forms) that was removed using filtering algorithms. After testing a variety of methods with different settings, it was decided to use a Majority filter from SAGA with a window size of 3*3 and then to filter resultant rasters once again with OTB

binary Morphological filtration operation Opening with Structuring Element Type – Ball, radius 5 pixels (fig.2.7).

5. Cleaned rasters were converted to polygons using algorithm GDAL “vectorize raster layer”.
6. Resulting vector layers contained the masks of all water objects (fig. 2.8 a,b). Both masks were combined to one single water body shapefile using the Dissovle function in GIS.

For the further analysis received files were divided on two types: the first one, layers, which contain isolated water objects or lakes, the second one layer that contains connecting river channels (fig.10). After splitting the whole water body dataset into these types, joined layers of RapidEye and SENTINEL-2 water channels and lakes (isolated water bodies) were created using QGIS and ArcGIS tools. Combination of two data sets provided several advantages. Using of SENTINEL-2 data allowed to cover gaps in RapidEye imagery and to get sharper water surface representation. On the other side RapidEye dataset provides more detailed scene and was better for shallow water classification.

Wherein in the layer with lakes were selected only objects with the size more than 100 m² and 99 objects with an area less this threshold were deleted. The total area of deleted features is about 0.002 km².

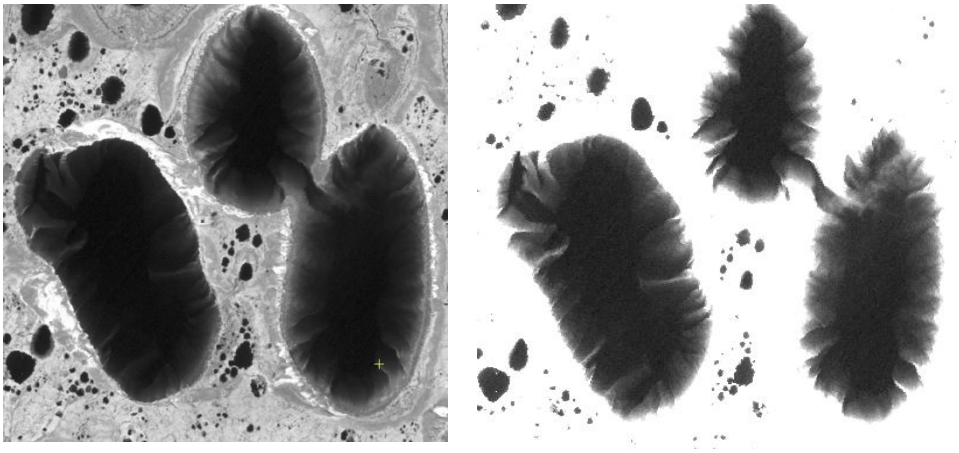

a b

c d

Figure 2.5. a. Lakes obtained by SENTINEL-2 in NIR channel; b. Lakes after application a r.series algorithm on SENTINEL-2 images in NIR channel; c. Lakes obtained after application of r.series algorithm on RapidEye images in NIR channel; d. Comparison of r.series algorithm results, (SENTINEL-2 image (2) situated inside RapidEye (1)

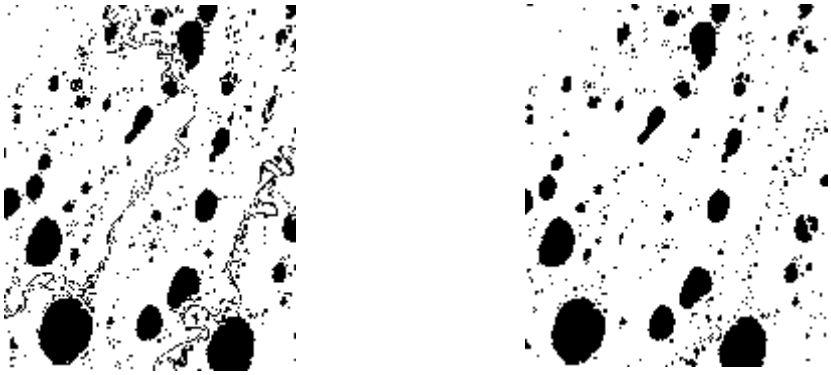

a b

Figure 2.6. Differences in resolving water body shape: a. Binary image based on RapidEye data; b. Binary image based on Sentinel data

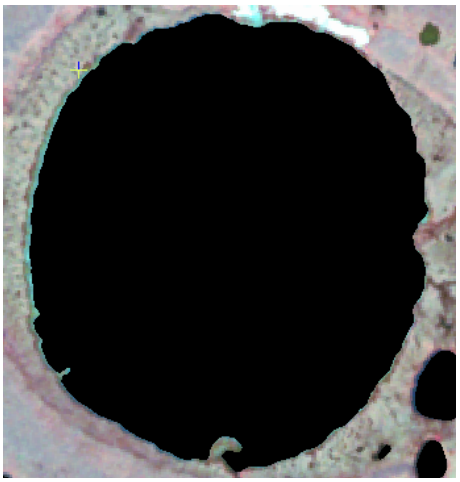

Figure 2.7. Lake on SENTINEL-2 image covered by mask, filtering method (SAGA majority filter window 3*3 pixel)*OTB binary morphological filter opening with structuring element ball with r=1

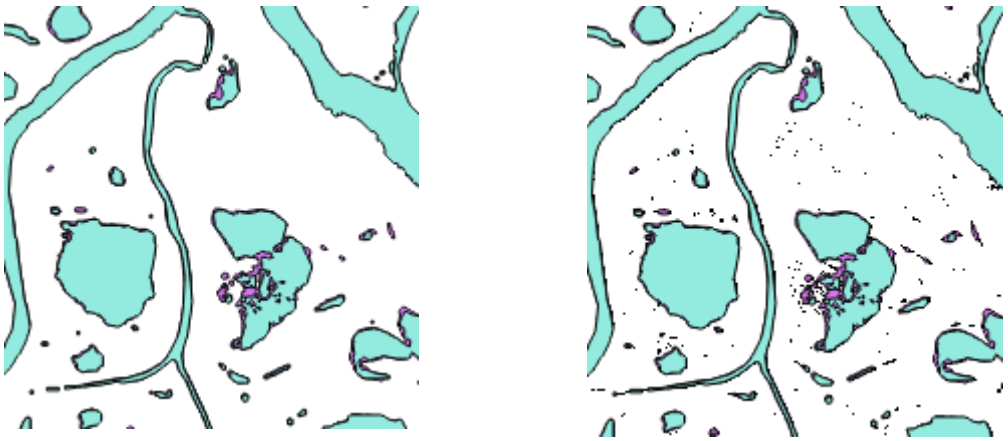

a b

Figure 2.8. Comparison of obtained masks with input raster data (scale 1: 50 000). Cian masks based on the SENTINEL-2 imagery, magenta – based on the RapidEye imagery. a. Pure masks; b. Masks superposed on the input raster data, where small dots – pixels of water on the input raster, that were excluded as result of the filtering

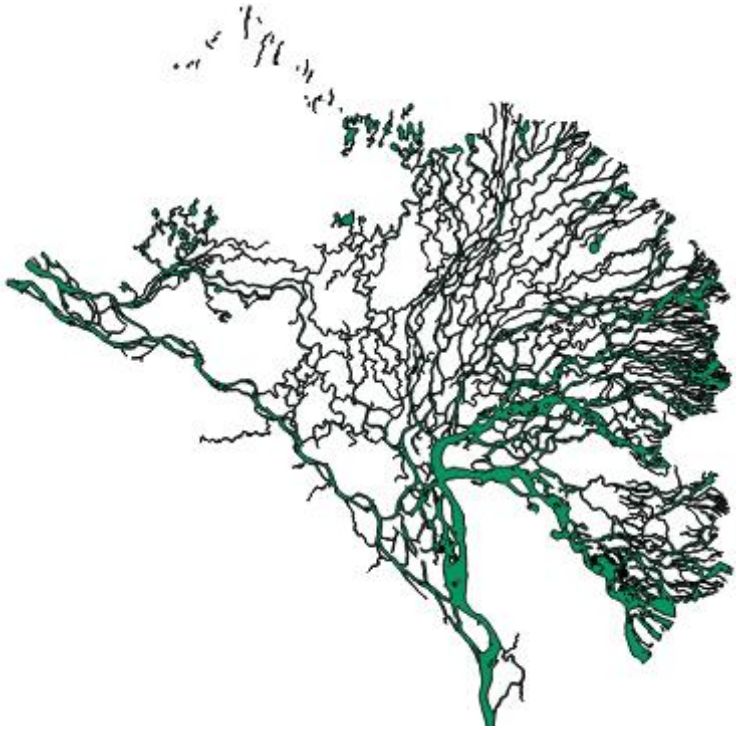

Figure 2.9. Vector scheme of main river channels of the Lena Delta. Scale 1: 2 500 000

2.2.3. DEM refinement

The TanDEM-X DEM is not hydrologically corrected and is not edited for water surfaces. This results in very noisy water level elevations in the DEM. Therefore, the very detailed vector mask of water bodies was used to edit heights of the lakes level in the DEM. To improve the height values for lake surfaces the following method was

applied. From the lake layer only objects with an area more than 1000 m² were selected, to edit areas of lakes location on TanDEM-X DEM using the DEM editing toolbox in Geomatica. The target of editing was to remove all bumps and pits by leveling and interpolating accurate heights along the shoreline over the surface of lakes. By this approach it has been possible not just to average wrong elevations of the lake surface, but to use the precise elevations of the lake margins and then to fill lakes surfaces with values from the edges of the polygon (PCI, 2015). Thus was used a following sequence of processing: "Remove Noise" – "Remove bumps" – "Remove pits" – "Fill from edges". The size of the filter box was set as 10 pixels.

To refine surfaces of several prominent water objects were manually rectified shorelines polygons to avoid mistakes and applied method "Opposite ends fill". The filter examines the selected polygon on each short end and finds an average elevation for each to use them in an interpolation (PCI, 2015).

2.2.4. Computation of characteristics

To extract elevation values from the DEM and connect them with appropriate polygons in vector layer, that display water objects was used operation QGIS "Zonal statistics", which computes: minimum, mean, maximum values, mode, median, standard deviation, count of cells, quantity of unique values of cells, and other parameters inside zones of interest. Also for all lakes were derived areas and perimeters.

Worth saying that despite of refinement of water surfaces on the DEM, it wasn't possible to get unique height values for appropriate lake. Consequently it was necessary to select the most plausible way for heights definition.

Highly important step of this study was estimation of elevation data extracted from the DEM and the choice of the most realistic value of lakes level height, calculated from the DEM. For this objective were used laser altimetry data. GLAS data provided by AWI were stored as vector layer with 104485 polygonal footprints of measurements for the entire Lena Delta. To avoid influence of snow cover on altitude measurements for the further analysis were selected only data obtained in period from the end of September until the end of November (Laser identifiers: L2A, L3A, L3D, L3G, L3I). By means of GIS spatial query were acquired only laser altimetry footprints falling into the lakes. The square of measurement footprint is about 3800 m², all footprints with an area over water surface < 3000 m² were excluded in case they fall into water – land

area. Thus were obtained 2985 elevation values for 762 lakes. For the large lakes with several altitude measurements were calculated mean values.

F. Günther proposed three options for heights calculations (personal consultations) on the basis of DEM data:

$$1.\ h = \bar{x};\ \ 2.\ h = \bar{x} - \sigma;\ 3.\ h = Me - \sigma,$$

where: h – assumed lakes level height, $\bar{x}$ - mean value for each lake, σ – Standard Deviation (std), Me – median.

Thus were obtained three sets of heights extracted from DEM and one set received by laser altimetry (accepted for the standard). Pair comparison between these series and their accuracy evaluation showed that elevation calculated as difference between mean values and std is the most similar to laser altimetry data.

Table 2.4. Comparison of laser altimetry and DEM data

	$\bar{x} - \sigma$	$Me - \sigma$	$\bar{x}$
Sum of elevations, m	694.16	699.95	925.0908
Root Mean Squared Error	0.9544	0.9584	1.1018
Correlation	0.9747	0.9746	0.9712

Mentioned above supposed receiving of real heights of water surfaces, that should be close to the shore line minimum elevation.

3. Results

Analyses of the results are based on a GIS layer (ESRI shape file), which contains the shape of all water objects. Furthermore, a comprehensive attribute table stores all relevant information on lake area, elevation above sea level and the assignment to particular river terrace. As a result, 198851 features including ponds, lakes, river channels with a size of more than 100 m² and 118947 features with an area of more than 1000 m² were obtained for the whole Lena Delta including Bykovsky Peninsula.

Figure 3.1 shows the complete scheme and spatial distribution of water objects. There were found 189497 ponds and lakes with the size more than 100 m² including 118224 objects with an area more than 1000 m² and 29631 lakes of more than 1 ha. These objects were then investigated in more detail. A total area of the watercourses in the delta mapped in this study is about 4237 km². Moreover a total length of channels in the Lena Delta, which is about 13132 km (12819 km belongs to Lena River distributaries), was calculated using acquired map of water objects.

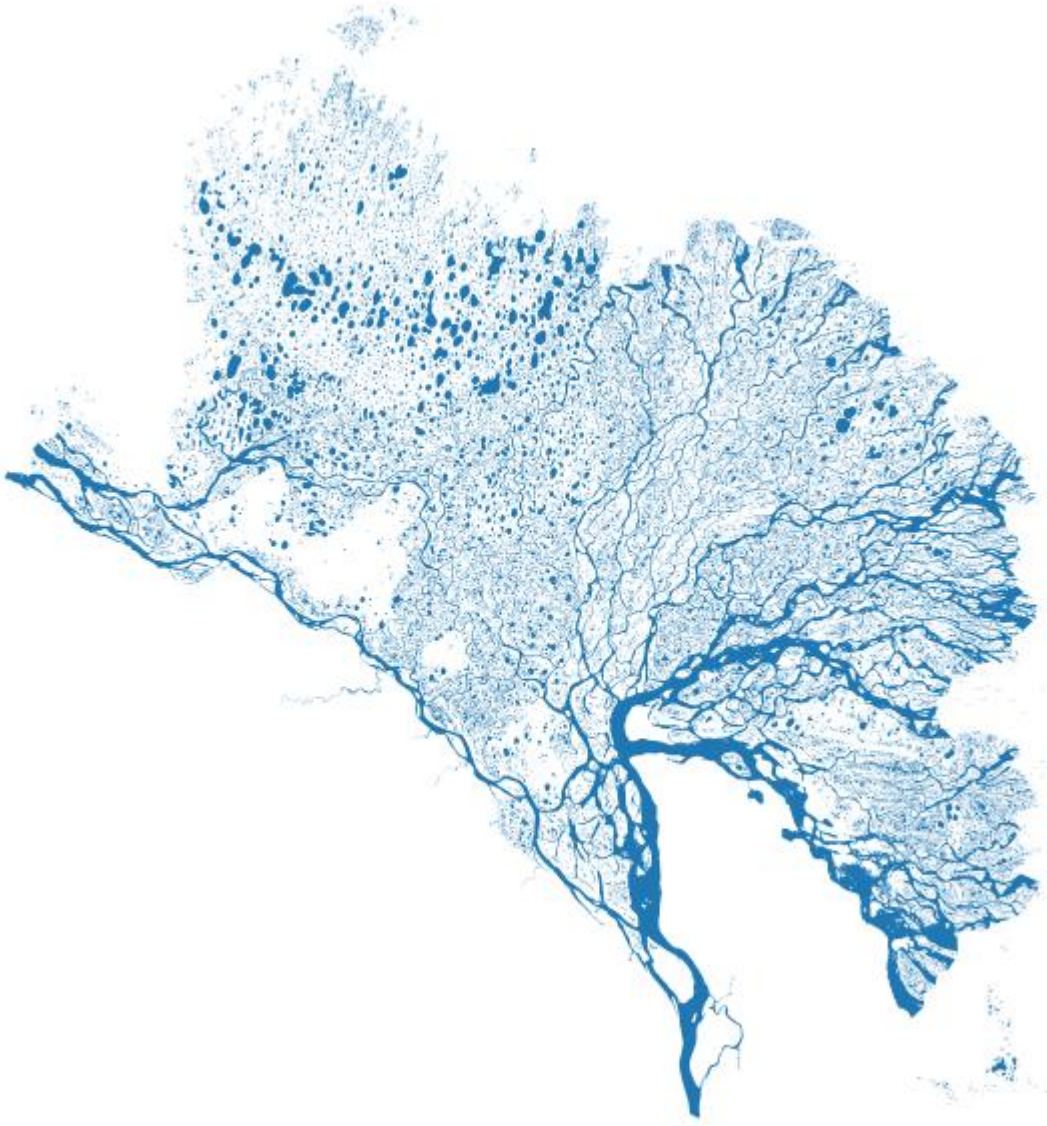

Figure 3.1. Vector scheme of water objects of the Lena Delta and Bykovsky peninsula.
Scale 1: 1 750 000

3.1. Spatial statistics

The total area of 189 497 lakes >100 m² found within the study area (the Lena Delta including the Bykovskij Peninsula) amounts to 3408.06 km². Out of this, 188 968 lakes with an area of almost 3390 km² are situated within the actual delta extend, meaning that 11.74 % of the delta are occupied by lakes. For further analysis, the Lena Delta area according to Schneider et al. (2009) (29036 km²) was taken, which is considered as 98% of entire area (Bolshiyanov et al., 2013), excluding the most southern apex of the delta that is not covered by the DEM used in this study. Distribution of lakes across the delta with respect different terrace levels is provided in table 3.1.

Tab. 3.1 Spatial distribution characteristics of lakes in the study region

	Total lakes area [km²]	**Number of lakes**	**Percentage of lake number fraction [%]**	**Area of terraces [km²]**	**Areal fraction of lake coverage per region[%]**	**Percentage of lake areal fraction[%]**
Entire Lena Delta	3408.02	188966	100	23813**	11.7%	100
First terrace	2239.8	132798	70.3	15840.1*	14.1%	65,7
Second terrace	1052.19	52158	27.6	6098.6*	17.3%	30.9
Third terrace	97.86	4010	2.1	1711.6*	5.7%	2.9
BYK***	16.41 (18.17)****	345 (526)****		172.5***	9.5%	

*According Morgenstern, (2005); ** According Schneider et al., (2009); ***Bykovsky Peninsula according Grosse et al., (2005); **** with adjacent part of Khorogor Valley

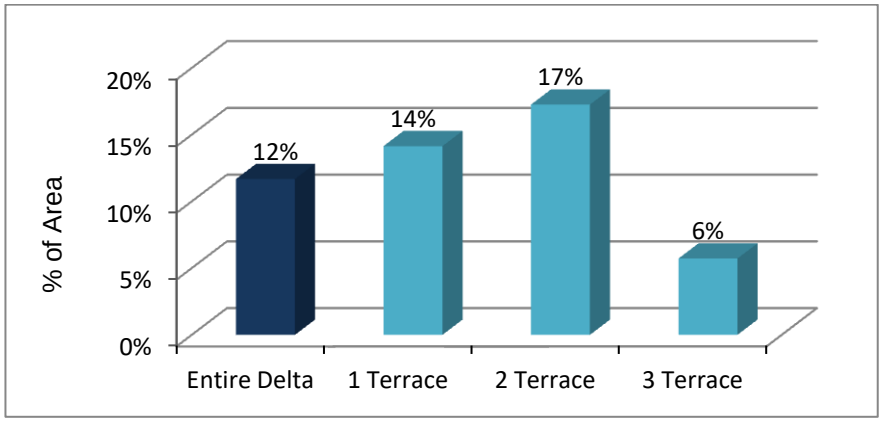

Figure 3.2. Percent of total terrace area covered by lakes

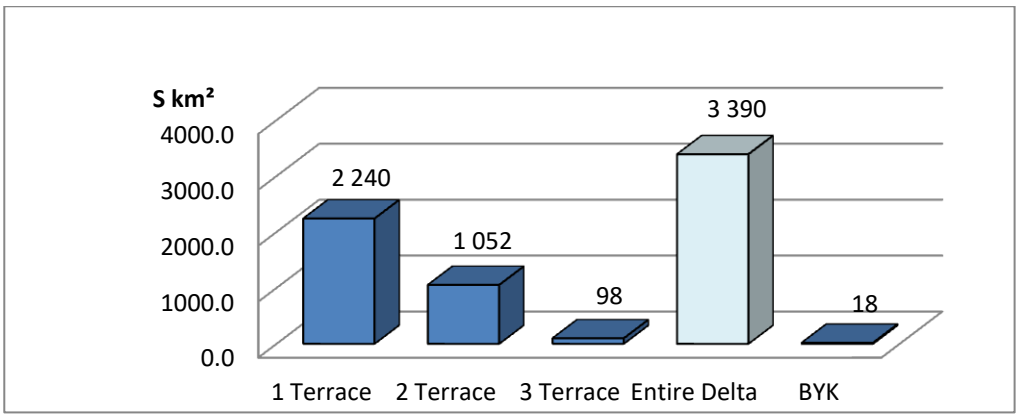

Figure 3.3. Lakes covered area by terraces. BYK – Bykovsky peninsula

The results show that percentage of the Lena Delta territory covered by lakes is 12%. This areal fraction is considerably higher than, for example, the percent of territory covered by lakes in Russia is near to 2.5% (http://water-rf.ru). Among the Lena Delta terraces, values are particularly high for the first and especially for the second terraces (tab. 3.1, fig.3.2). The percentage of open water covered area on the third terrace is much lower in comparison with the whole Lena Delta. In absolute terms, the greatest contribution to the lacustrine area is due to the first terrace with almost 133 000 of lakes covering a total area of 2240 km². Although 70% of the total amount of lakes is concentrated on this terrace, their areal fraction is somewhat lower at around two-third of the total lake area in the Lena Delta (fig. 3.3, tab. 3.1).

Tab 3.2 Statistical characteristics of the lakes elevation and area by terraces in the Lena Delta

	1st terrace		**2nd terrace**		**3rd terrace**		**entire Delta**	
	area, m²	elev., m	area, m²	elev., m	area, m²	elev., m	area, m²	elev., m
mean	16866.3	4.4	20173.1	8.9	24402.9	20.3	17938.9	5.9
std	114026.4	3.3	267460.4	6.2	136179.4	11.8	171109.1	5.5
median	1550.0	3.8	1625.0	8.0	1600.0	19.0	1575.0	4.6
max	2239.8		1052.19		2584500.0	64.3	24318275.0	64.3
min	125.0	0	125.0	0	225.0	0	125.0	0.0

Tab 3.3 Statistical characteristics of lake elevations and surface areas on Bykovsky Peninsula

	area, m²*	elevation, m*	area, m²	elevation, m
mean	34538.6	8.6	47592.1	10.5
mode	400.0	0.0	400.0	3.1
std	273113.7	10.8	335739.9	12.6
median	2550.0	3.4	2550.0	3.4

max	5903000.0	40.2	5903000.0	40.2
min	225.0	0	225.0	0

* including adjacent part of Khorogor Valley

As described in the methods, this study only considers lakes with an area of more than 100 m², because of technical and methodical limitations. Average lake size in the study region is about 1.8 ha, while maximum size is up to 25 km² (tab. 3.2). The high standard deviation of ±17.1 ha is also reflected in a considerably lower median size of 1.6 ha. The third terrace is characterized by the largest (24.4 ha) and the first terrace by the smallest mean size of lakes (16.9 ha). However, the median size is relatively similar across all terraces. Standard deviations of lakes areas are highest for the second terrace two times higher as for other terraces moreover it is quite high when considering lakes of the entire delta.

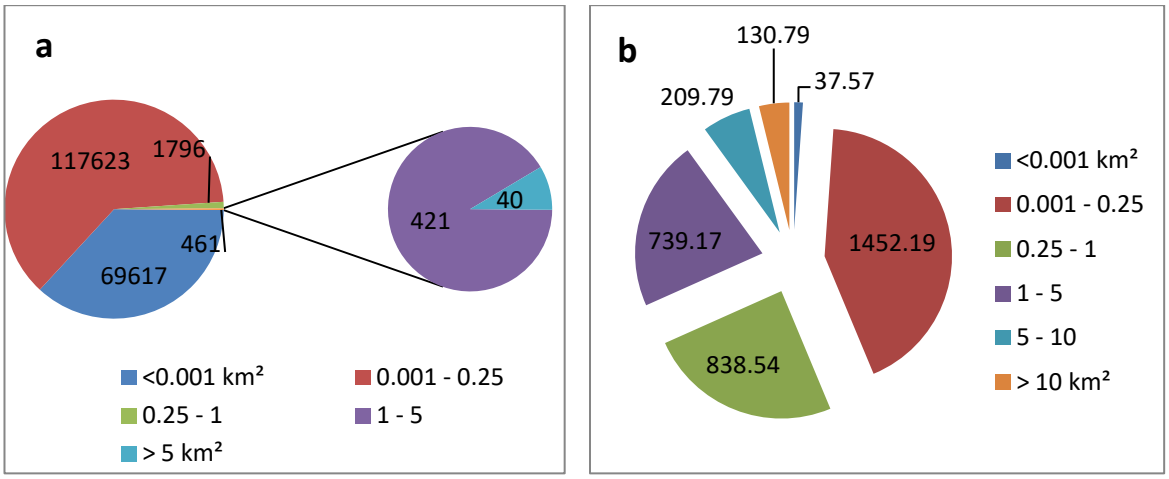

Figure 3.4. Lakes mirror size in the Lena Delta and Bykovsky Peninsula. a – number of lakes in each group relatively to lakes area. b. Lakes covered area relatively to lakes area (1 <0.001 km²; 2. 0.001 – 0.25 km²; 3. 0.25 - 1 km²; 4. 1 – 5 km²; 5. 5 – 10 km²; 6. > 10 km²)

General distribution of lakes area over the entire Lena Delta is displayed in the Fig.13. Grouping by area for analysis is based on Bolshiyanov et al. (2013) with adding a special group of lakes with area under 1000 m². Majority of lakes in the delta 117623 have an area between 0.25 - 1 km² (fig.3.4a). Herewith only a minor part of lakes can be considered as large, with an area more than 1 km². Fig. 3.4b shows that although quantity of ponds and small lakes in the first group stays on the second place, an area which is covered by this group is least in comparison with other groups. For the second group the number of lakes correlates well with a territory occupied by this group. It should be noted that small number of relatively major lakes plays a great role in the

water area distribution. For example number of lakes in the third group is about four times more than in the fourth group, but values of filed areas are very similar.

Distribution territory covered by lakes relatively to terraces is considered (fig.3.5) according grouping of lakes area based on the work of Boike et al. (2013), where lakes divided on three groups according area: polygonal ponds, polygonal lakes, thermokarst lakes. In this work one more category is added: large thermokarst lakes, with an area of more than 1 km². The major area is occupied by thermokarst lakes (third group) for total area as well as for the first and the third terraces. Moreover area of the third group exceeds a total area of other groups, for the third and first terraces as well as in general. The second terrace differs from the other terraces, because major part of the entire lake area is occupied by large lakes with an area more than 1 km². However, figure 14 demonstrates that the largest amount of all lakes is situated on the first terrace, across all lake size classes.

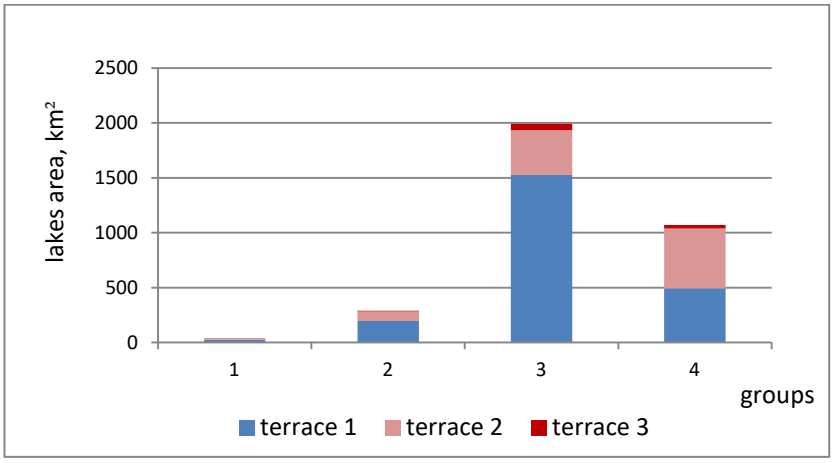

Figure 3.5. Distribution of territory covered by lakes relatively to 4 lakes size groups and terraces. 1. area <0.001 km² (polygonal ponds); 2. 0.001 – 0.01 km² (polygonal lakes); 3. 0.01 - 1 km² (thermokarst lakes); area>1 km² (large thermokarst lakes)

The most common lake size all over the delta generally as well as separately for each terrace are polygonal lakes according to classification of Boike et al. (2013), which have an area between 1000 m² and 1 ha (fig. 3.6). Especially on the first and particularly on the second terrace they account for around a half of all lakes, with 45.8% and 52%, respectively (fig. 3.6). Water bodies from the third and the fourth groups with an area of more than 1 ha (thermokarst lakes) are relatively sparse (fig. 3.6), only 29541 from 188968 lakes in total within the delta, according to 16%. However, as it was mentioned before they are responsible for the majority of areal lake coverage in the delta (fig.3.5), where 3060.9 out of 3389.89 km² are covered by these lake types, corresponding to 90%

areal fraction. In contrast, small water bodies like ponds with an area between 100 m² and 1 ha occupy the smallest territory despite of their number, where a huge amount of polygonal lakes with 48% of all lakes in delta corresponds to a relatively small areal fraction of only 9%. The shape and the size of polygonal ponds are defined by ice-wedge structures (Boike et al., 2013).

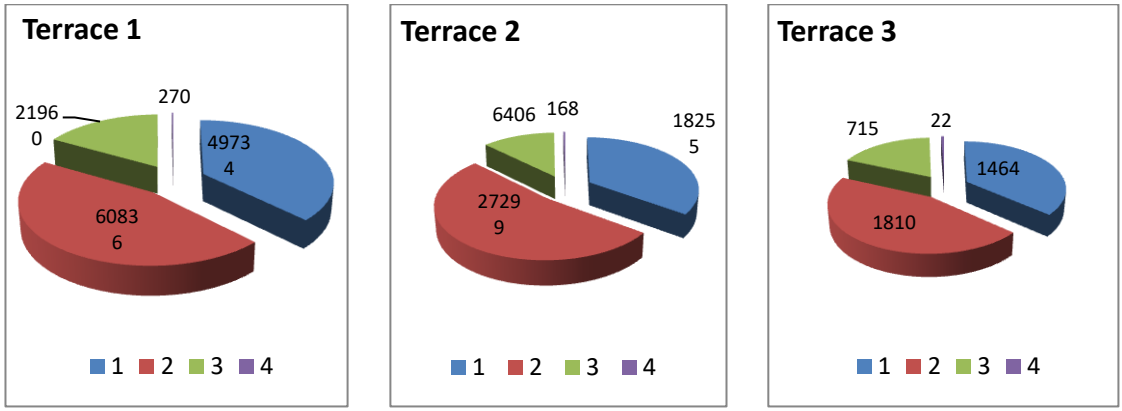

Figure 3.6. Number of lakes by size. Groups: 1. area <0,001 km²; 2. area between 0,001 and 0,01 km²; 3. 0,01 and 1 km²; 4. area>1 km²

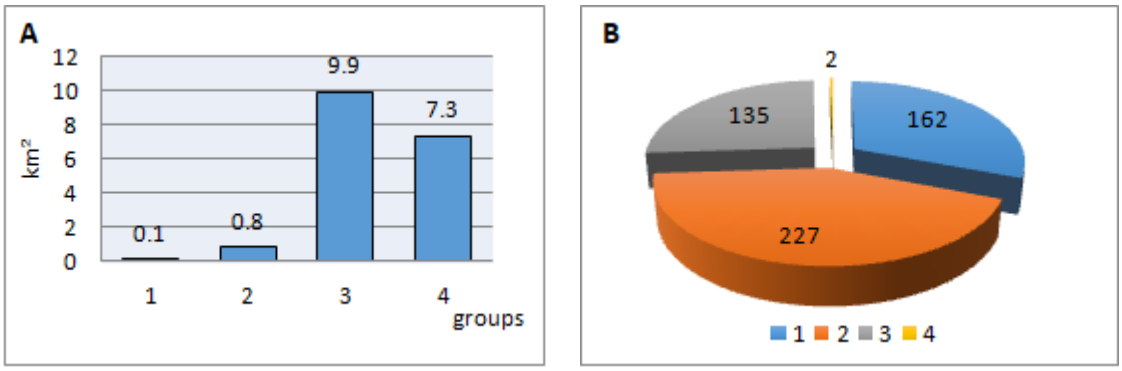

Figure 3.7. Distribution of lakes by area on Bykovsky Peninsula A: Total lakes area for each group; B: Number of lakes in each group. Groups: 1. area <0,001 km²; 2. area between 0,001 and 0,01 km²; 3. 0,01 and 1 km²; area>1 km²

Lakes on Bykovsky Peninsula were considered together with Lena Delta. Figure 3.7a shows that the distribution of lakes by groups on the base of covered area as well as distribution of groups by quantity of water bodies in each group is similar to allocation in Lena Delta (fig.3.5; 3.6). On the other side relative quantity of polygonal lakes is higher comparatively to Lena Delta terraces.

3.2. Lake height distribution

For all lakes their water level height was evaluated based on a TanDEM-X digital elevation model with 12m spatial resolution. The results of statistical analysis (mean, median and std values) of lakes elevation generally reflects all terrace levels of the Lena Delta. Figure 3.8 shows that lakes on the third terrace lay above lakes from the second terrace which lay consequently above lakes from the first terrace. For the first time, this work determines that mean elevation of all lakes in the Lena Delta is about 6 m above sea level. For the third terrace, which is according Are and Reimnitz (2000) 20 – 60 m high coastal plain composed from ice-complex deposits, median lake elevation is about 19 m (tab. 3.2). Mean elevation of lake water levels on the 20 - 22 m high sand terrace (Are and Reimnitz, 2000) or the second terrace is about 9 m (tab. 3.2). Finally mean lake water level of the first terrace is about 4.5 m.

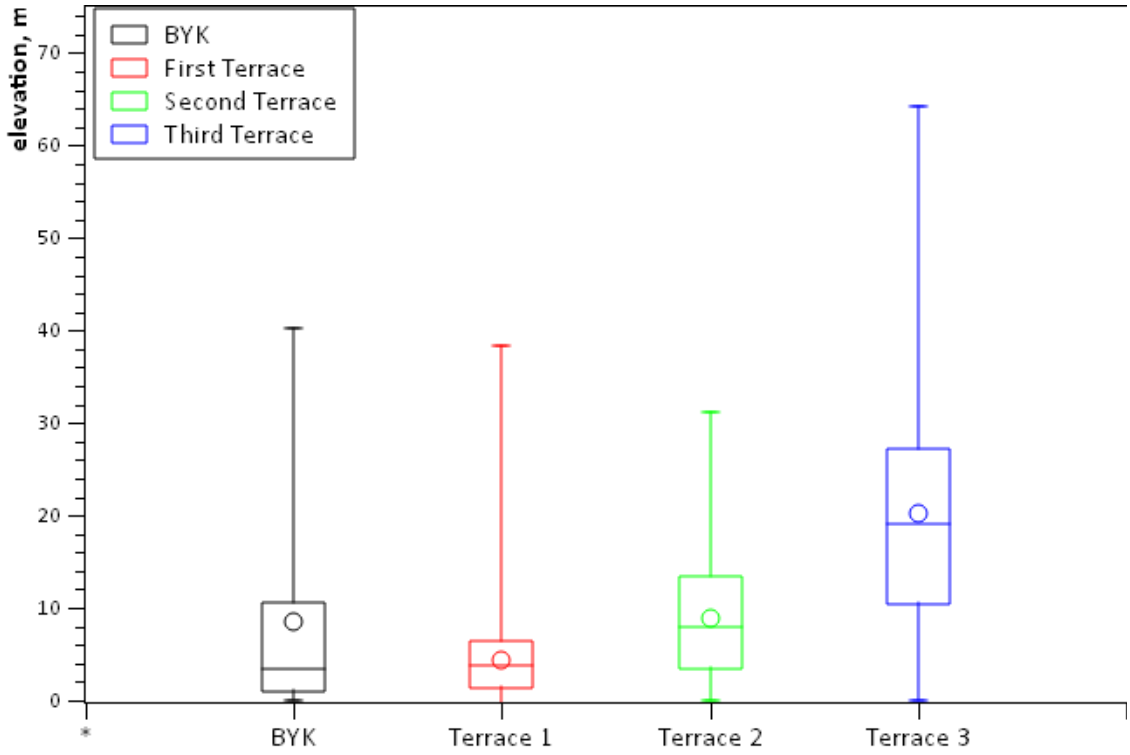

Figure 3.8. Statistical distribution of lakes level elevations corresponding to terraces. Inside boxes – 2nd and 3rd quartiles (25-75%), whiskers - max and min values, circles – mean values; BYK – Bykovsky Peninsula

Statistical characteristics of lake elevations display noticeable differences between the main geomorphological elements of the study area, including three terraces in the delta and the Bykovsky Peninsula. Based on figure 17 it is obvious that distribution interval of lakes elevation values is greatest for the third terrace and the maximum elevation of lakes water level is above 64 m. Even 50% percent of central values show notable scattering. Moreover significant distribution and heights can be

observed on the Bykovsky Peninsula. This is of particular notice since the Bykovsky Peninsula geomorphologacally belongs to the third terrace (Grigoriev, 1993).

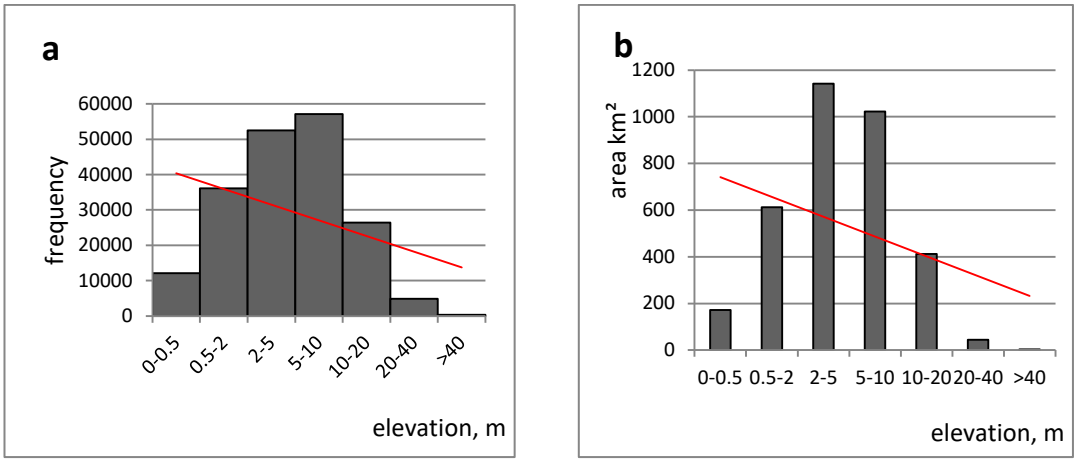

Figure 3.9. Histograms lakes and elevation. a – frequency of lakes relatively to elevation; b – area covered by lakes relatively to elevation. Red line - trend

Most often lakes in the Lena Delta and on Bykovsky Peninsula are located at heights between 2 and 10 m (fig.3.9 a, b). Mode for elevation for the entire Lena Delta and Bykovsky peninsula is 0 m Exception is the third terrace, where mode for elevation is more than 18 m. Only relatively few lakes are situated at heights above 40 m. On the other side more than 10000 ponds and lakes are located at heights under 0.5 m. The highest lake situated on the third terrace on the elevation of 64.3 m. The highest lake on Bykovsky Peninsula has an elevation above 40 m. General trend shows moderate decrease of lakes number with increasing height. Decreasing of area covered by lakes with elevation trend is slightly steeper. The pattern of lake area relative to elevation (fig.3.9b) generally matches with the number of lakes relative to elevation (fig.3.9a). However, the largest area is occupied by lakes with an elevation between 2 and 5 m.

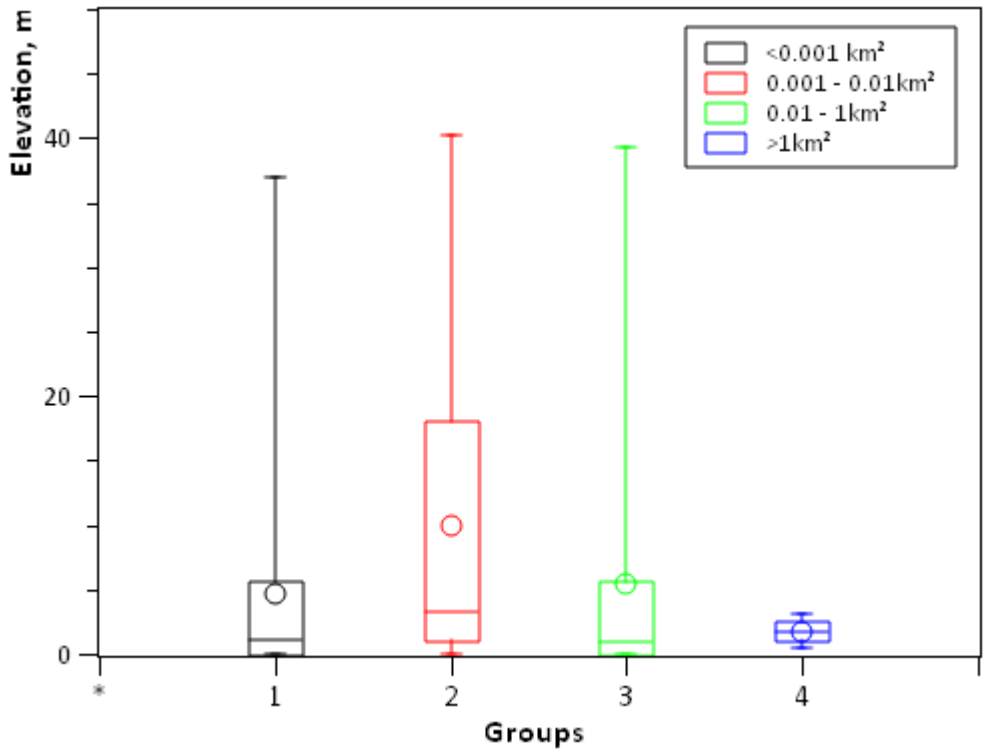

Figure 3.10. Distribution of lakes by elevation on Bykovsky Peninsula. Boxes – 2nd and 3rd quartiles (50% of data), whiskers – 3 max and min values, circles – mean values. Groups: 1. area <0,001 km²; 2. area between 0,001 and 0,01 km²; 3. 0,01 and 1 km²; area>1 km²

Statistical characteristics, which exhibit the relation between lake elevation and lake size were evaluated on the example of Bykovsky Peninsula (fig.3.10). Lake positions according to water level heights in all groups show significant dispersion. Roughly average height of lakes doesn't depend on lakes size, for all groups mean elevation is approximately equal and is about 8.5 m (tab. 3.3). Median heights of each group are considerably lower than the mean and almost identical and close to 3.5 m (tab. 3.3, fig. 3.10). However, at the same time polygonal lakes (second group) show larger variety and are generally situated a bit higher, then lakes from other groups.

3.3. Vertical section of the Lena Delta based on the lakes level heights

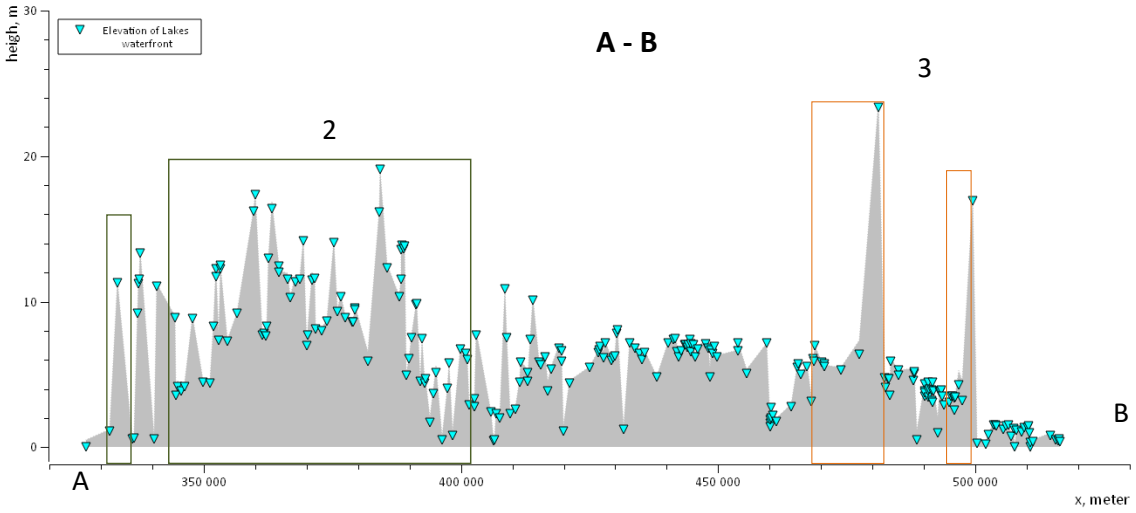
A - B
Elevation of Lakes waterfront
height, m
30
20
10
0
2
3
A
B
350 000
400 000
450 000
500 000
x, meter

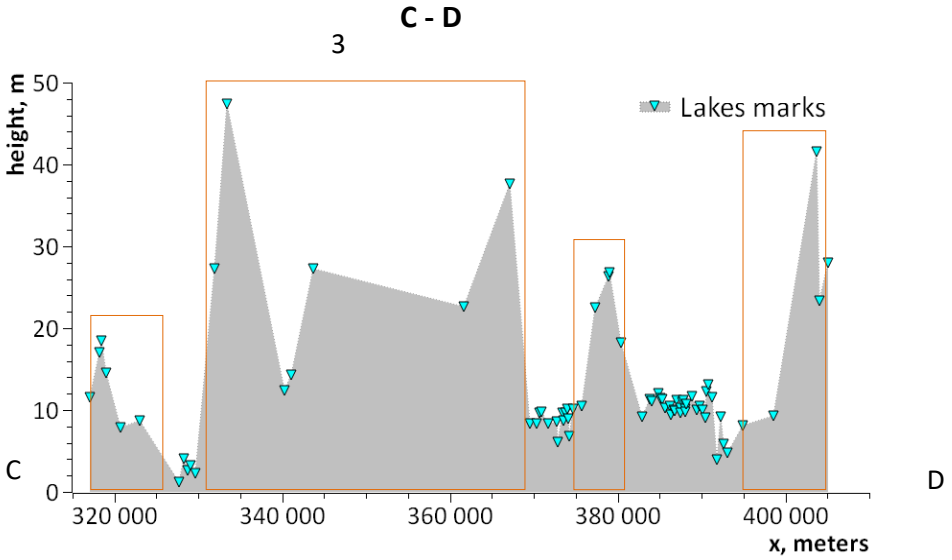
C - D
3
height, m
50
40
30
20
10
0
Lakes marks
C
D
320 000
340 000
360 000
380 000
400 000
x, meters

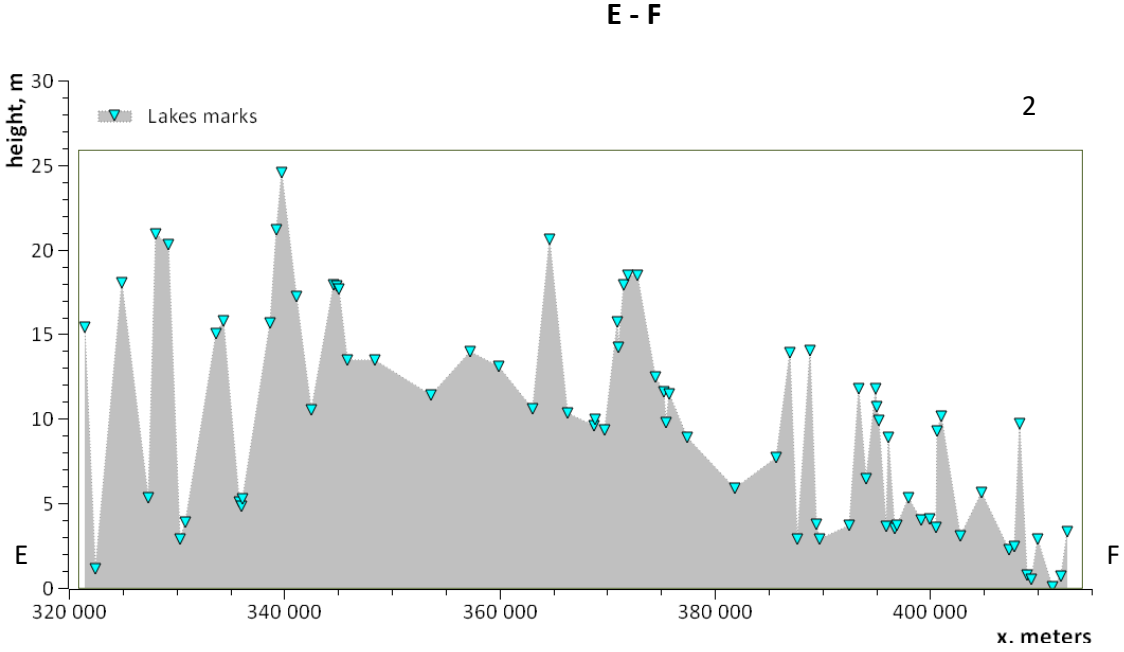
E - F
height, m
30
25
20
15
10
5
0
Lakes marks
2
E
F
320 000
340 000
360 000
380 000
400 000
x, meters

1

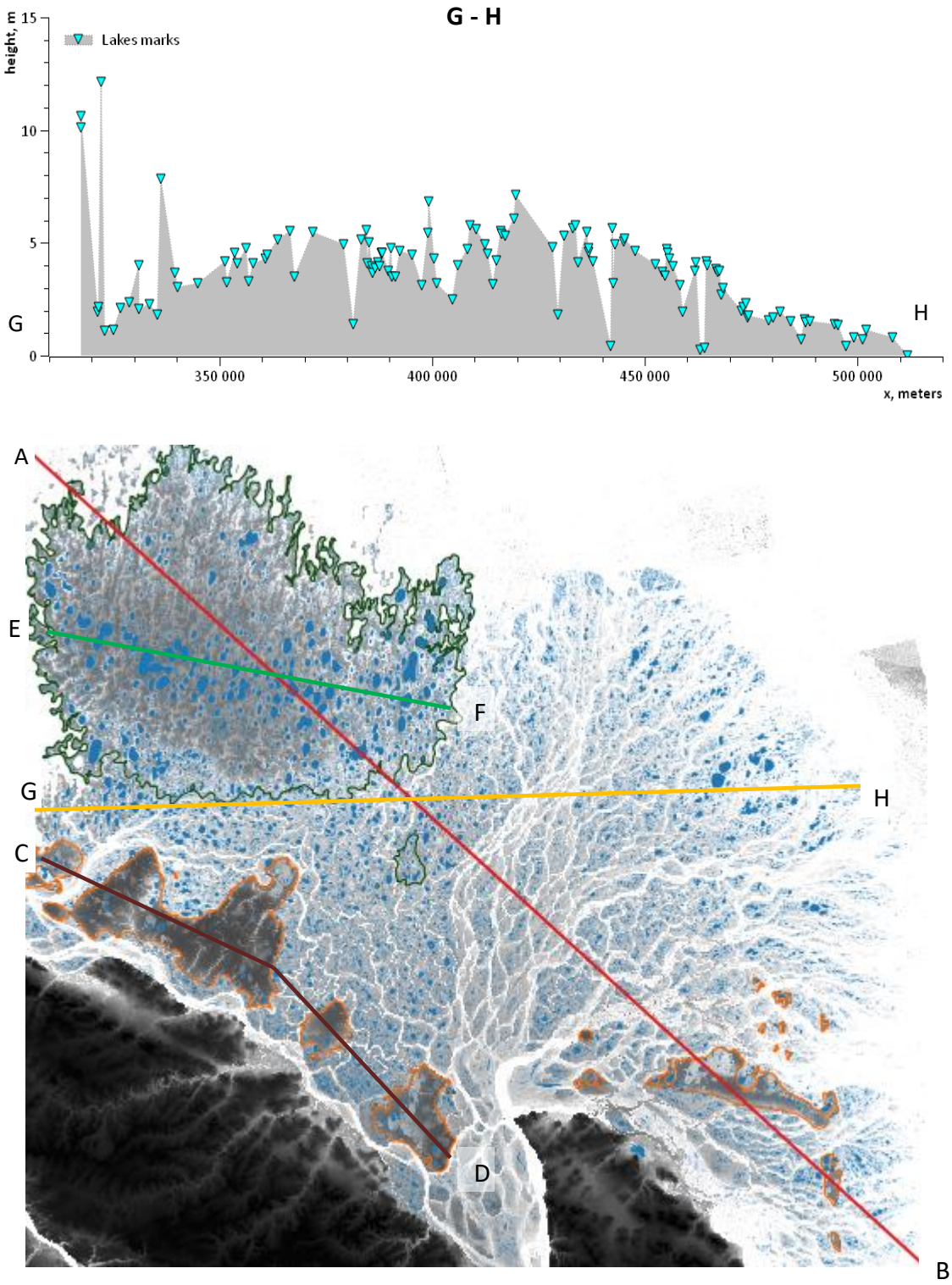

Figure 3.11. Profile of lakes elevations. Top: vertical sections, turquoise triangles – lakes position: a. A – B the entire delta; b. C-D 3rd terrace section; c. E – F 2nd terrace section; d. G – H 1st terrace section. Red – profile line; green – second terrace border; orange – third terrace border. Bottom: plane section

In order to display the variability of the Lena Delta topography with respect to its geomorphological structure, a section presented in figure 3.11, which crosses all terraces in the Lena Delta in the direction from the North–West to the South-East and

separately each terrace from West to East shows significant scattering of lakes elevations over the entire area. On the other side each terrace can be distinguished on the basis of this chart. Especially prominent on this graph is Arga Island in the north-western part of the delta, which builds up the second terrace. Sobo-Sise Island (third terrace) in the eastern part of the delta is also well distinguishable on the profile. The areas in between show pretty well the general elevation decrease of lakes water in the central part of the first terrace towards the sea shoreline at the eastern margin of the delta.

4. Discussion

4.1. Applicability of remote sensing data processing and GIS methods for creation of water objects scheme

Preprocessing of satellite images, difficulties and uncertainties

Set of high-resolution satellite images provides a new opportunity for creation a precise map of thermokarst affected landscapes over the whole Lena Delta in comparison with coarser Landsat images, usually used for this objective (Schneider et al., 2009), (Kravtsova and Rodionova, 2016), (Nitze and Grosse, 2016), which can be used for the further analysis of origin and dynamics of area of interest. This can be explained by the relation between the spatial resolution and number of landscapes forms. The higher the spatial resolution is, the more lakes can be observed. Therefore in our study important factors for the satellite images selection were:

1. Full cover of the region of interest;
2. Display of suitable situation of landscape.

In order to cover the entire Lena Delta in this study to the main set of high-resolution RapidEye images was added set of SENTINEL-2 images with coarser resolution, which was later enhanced automatically. Thus in order to get a scheme of water objects two sets of data with different initial resolution were compiled consequently with different detailing (fig. 4.1).

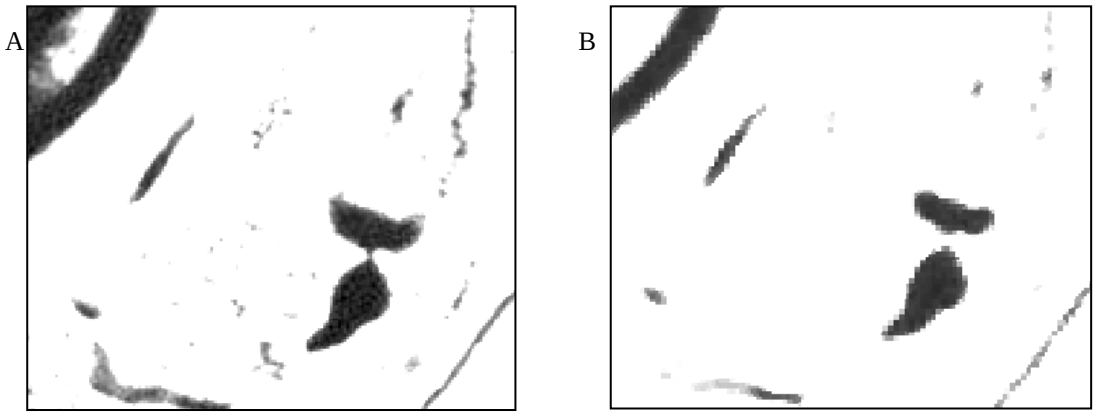

Figure 4.1. Different accuracy of surface display. A – RapidEye dataset; B – SENTINEL-2 dataset

Within this study was used overlay of near-infrared channels from RapidEye and SENTINEL-2 sets from July, June and beginning of September from different years. Thus, the overlay provides generally snapshot of the maximal water expansion in the

end-summer situation, when the discharge is low during 2009 – 2016 years, which helped to avoid problems with water classification due to remains of ice, pointed by Grosse et al., (2008). As in study by Schneider et al., (2009) in this study was not correctly considered seasonal variability of water level, which is maximal in May – June and minimum during winter months. According to Grosse et al., (2008) seasonal hydroclimatology can have a prominent effect on lake surface area for lakes with shallow basin topography mostly ponds. On the other hand thermokarst lakes typically can be determined by steep banks and a more pronounced basin morphology, which limits lateral surface changes due to seasonal vertical level variations (Grosse et al., 2008).

The study area has a large E-W extent and covers the 51N and 52N UTM zones. The UTM meridian is situated in the center of the Lena Delta. Despite of that all images in this project were orthorectificated and projected in the Universal Transverse Mercator (UTM) projection Zone 52N because main part of images and already rectified images GeoEye with ground control points were situated in this zone. Such decision negatively influenced on the further morphometric calculations in the western part of the Lena River Delta. To minimize distortion effects on morphometric calculations Morgenstern, (2012) separated the data set along the UTM meridian into a western and an eastern part and reprojected western part to its original UTM Zone 51N for mapping. Such action wasn't done in this study because of huge amount of data (obtained objects).

Preprocessing of images for further mosaicking commonly includes atmospheric correction to lead values of pixels to Digital Numbers (DN) – real reflectance value of surface. Nitze and Grosse, (2016) used for classification top of atmosphere reflectance values. In this study were used ground reflectance values. In order to obtain these values there were applied several models of this correction including removing of clouds and haze. Due to problems of algorithm to distinguish river sandy river deposits and haze (fig.5), and problems with recognizing of other completely different objects with similar reflection, it was decided to use corrected images without masking. As result of atmospheric correction were obtained different DN for the same area for RapidEye and SENTINEL-2.

The most common method for a general land cover classification of large heterogeneous datasets is the automatic unsupervised classification based on a chain algorithm and the consecutive labeling of land cover classes with real land cover features (Schneider et al., 2009). But to distinguish wetlands Schneider et al., (2009) used supervised classification approach based on a small number of classes. Grosse et

al., (2008) applied a simple density slice classification to distinguish water and land in the panchromatic imagery. To extract water bodies automatically from the Landsat-7 ETM+ image mosaic of the Lena River Delta, Morgenstern (2012) applied a grey-level thresholding on mid-infrared band with threshold values of top-of-atmosphere reflectance of 0 to 0.1. In this study also was tried to produce different methods of supervised and unsupervised classification over the mosaic created on the basis of RapidEye images in order to extract water bodies. Such classification results gave unsatisfactory results, because of misclassification of moist or slightly flooded river deposits -sand islands or beaches on the first terrace of the Lena River Delta resulting in lower DN due to low water reflectance. Lakes influenced by shallow water levels (probably less than 1 m), resulting in higher DN were misclassified due to reflectance of the lake bottom, or due to turbid water with high sediment suspension, resulting in higher DN from the sediment load (Grosse et al., 2008).

Thus, taking into account previous study designated that in near and mid-infrared wavelengths water bodies are strong absorbers, easily distinguishable from other land cover types (Morgenstern, 2012), overlay of near-infrared bands of images was carried out at which each output cell value was set as a minimum value of the values assigned to the corresponding cells in the input images. To extract water bodies was applied a grey-level thresholding with different threshold values for SENTINEL-2 and RapidEye imageries (values of 0.1 to 2.7 and of 0.1 to 8.8 correspondingly) due to difference in DN described above. Usually, there is a strong difference in reflectance in near-infrared band between water bodies (low DN displayed dark) and bare or vegetated land surface (high DN exhibited bright) (Grosse et al., 2008). Applied method has weak points, which lead to misclassified results in case of steep north-facing cliffs or slopes and deep thermo-erosional valleys, which was also considered by Grosse et al., (2008). More over Schneider et al., (2009) marked that vegetation either growing or floating in the lake can pose a challenge for any water-land distinguishing methods. They estimated the effect of unclassified water due to vegetation on the order of <2% of the overall water body area for some lakes. But in case of shallow or mud water classification based on minimum values in near - infrared channel fits enough.

Filtering of obtained mosaics

Filtering of binary mosaics in order to remove noises, enhance objects and get proper results in the further automatic raster to vector conversion is necessary (fig 4.2), when there is no opportunity to correct resulting vector layers manually due to a huge

amount of objects. In order to determine the best method of filtering a short study based on the visual evaluation of obtained results was carried out.

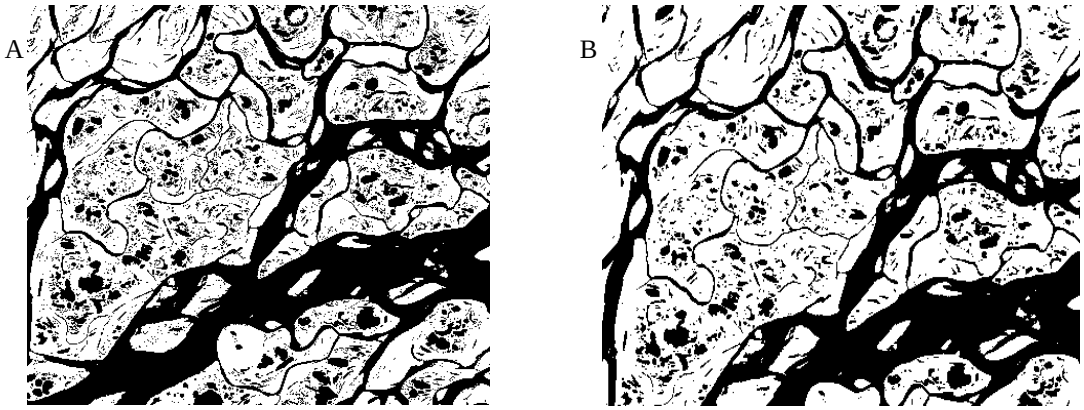

Figure 4.2. A - initial binary image based on RapidEye data; B - image after filtering (opening)

Main target was to select methodic of filtering, which removes noises and at the same time keeps important forms and narrow rivers channels. Morphological filtration was used as a basic type. The field of mathematical morphology contributes a wide range of operators to image processing, all based around a few simple mathematical concepts. Especially important are two operators: dilation and erosion, their join creates correspondingly opening or closing operators. Erosion shrinks an image by stripping away a layer of pixels from both the inner and outer boundaries of regions. The holes and gaps between different regions become larger, and small details are eliminated. Dilation has an opposite effect to erosion. Morphological opening of an image is defined as the dilation of the erosion of the image. The result is the reduction of small positive regions within the image. Morphological closing of an image is defined as the erosion of the dilation of the image, the result of closing is opposite to opening. Important settings are size and type of structuring element, which is used like filter window. For targets mentioned above the best operation is opening (fig. 4.3a).

When dealing with the Lena River Delta mosaic, it becomes apparent that there are very tiny water cluster within a single large land or vice versa. To remove such noise and to produce a more realistic scene, we decided to use the Majority Filter (SAGA) (fig. 4.3b), which considers all the pixels in the convolution window, and assigns the most abundant class in this window to the central pixel (Introduction to SAGA, 2017).

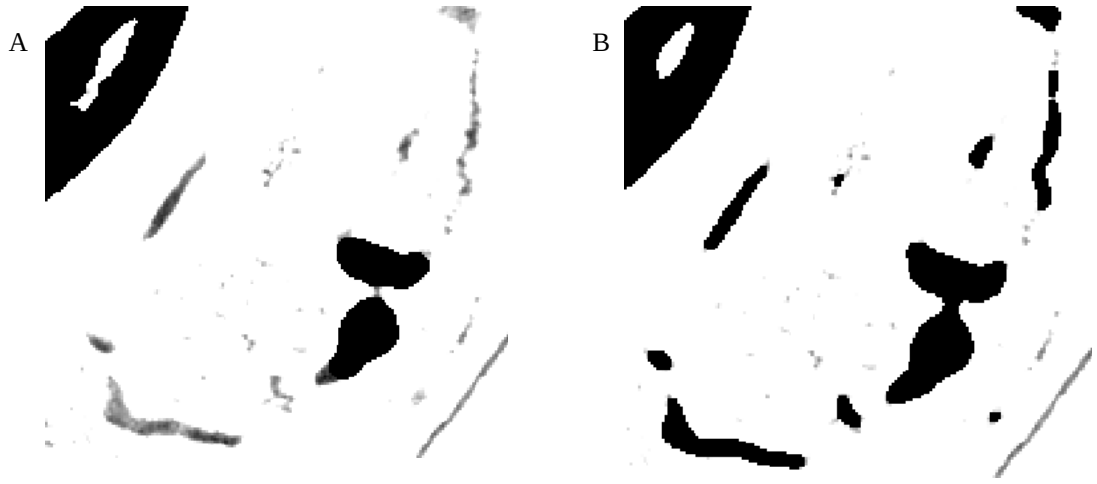

Figure 4.3. RapidEye initial mosaic covered by RapidEye filtered binary image. A - filter opening with structuring element ball, r=5; B – (majority filter window 3*3 pixel)*(filter opening with structuring element ball, r=1)

As the result of this study for the filtering was chosen method: (SAGA majority filter window 3*3 pixel)*(OTB binary morphological filter opening with structuring element ball with r=1) (fig 4.3).

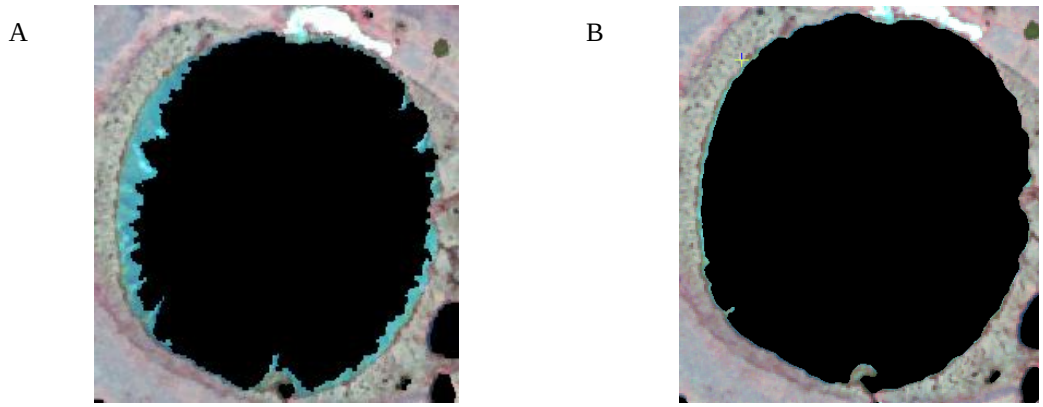

Figure 4.4. SENTINEL-2 image covered by water mask based on RapidEye image (A) and SENTINEL-2 image (B); filtering method (SAGA majority filter window 3*3 pixel)*(OTB binary morphological filter opening with structuring element ball with r=1)

Figure 4.4 shows significant difference between filtered mask based on the SENTINEL-2 images (fig.4.4, a) and based on the RapidEye images (fig.4.4, b). Reasons for this difference are able to be: a. difference of threshold values used to separate waters for SENTINEL-2 and RapidEye sets; b. Different levels of lakes due to different time of observations, SENTINEL-2 images were created at the beginning of September 2016, all RaidEye images were obtained in years 2009 – 2015. Different level of lake means relative significant changes of shallow water deep for the remote sensing, which leads to significant changes of DN and further misclassification.

After filtering of initial mosaic a river channels were partly divided in the narrow places. Thus were received additional lakes, which in fact are rivers, drainage channels, small streams or oxbows, but not lakes. Morgenstern in her study (2012) manually removed all such water pixels. In this work we also tried to correct resulted water scheme manually.

Water elevation extraction

For the analysis of lakes level heights in this study we needed to get value of averaged shoreline elevation for each water body. DEM presented water as very rough surface sometimes with significant height differences. To minimize these differences and to smooth initial DEM, water mask was corrected using different methods including interpolation of elevation values from polygon edges (shoreline). Obviously that such method supposed mistakes in case when polygon of lake situated incorrect. In some places such mistakes were manually fixed. Mean standard deviation of elevation value for lakes with raw (initial) DEM surface is about 0.22 and for lakes with smoothed surface is 0.15. Maximal standard deviation for smoothed lakes is =3.29 m, for non-smoothed 4.41 m, minimum STD for both is 0.

To estimate accuracy of obtained mean elevations for each lake they were compared with 77 elevations of significant lakes in various parts of study area, extracted from topographic map with terrain conditions on 1981 and scale: 1: 200 000. Mean Square Error (MSE) of difference between these two rows of data 7.6 m. MSE of difference between elevations from topographic map and mean elevation value from DEM minus STD of mean value for each lake is 4.5. Thus in this study was decided to use as elevations difference between mean height value for each lake and STD. This approach corresponds to the understanding that water level generally fits to the lower shoreline of water body. On the other side, hence thermokarst landscapes in the Lena River Delta are volatile, comparison of modern results with data obtained 30 years ago can bring mistakes.

Comparison of heights data calculated from DEM with altitude obtained by laser altimetry of GLAS/ICESat showed a correlation between two datasets with a coefficient near to 1. Thus convergence of elevation results confirms the possibility to use combination of edited DEM and GLAS laser altimetry data for the determination of inland water-edge.

One more weak point is that despite of corrections a lot of water bodies, derived elevation under 0. Majority of such lakes is situated near to the sea or in the river

channels valleys. Probably these values are caused by inaccuracy of used DEM water mask, especially for fluid water.

4.2. Discussion of obtained results

Entire study area

The Lena Delta as other Arctic deltas is characterized by an abundance of ponds and lakes. These ponds and lakes display highly varied sizes, shapes, depths, elevations and methods of formation (Walker H., 1998). Kravtsova and Bystrova (2009) marked that the region of the Lena River Delta is described relatively to the major part of Mid-East Siberia, by a concentration of lakes network and an increase in the size of lakes.

They are present in a variety of deltaic environments including old river channels (e.g., oxbow lakes), terrace-flank depressions, thaw depressions, inter- and intra-dune depressions, swales in ridge and swale deposits, low-centered polygons and the troughs between polygons.

An area of the delta covered by lakes obtained in this study is a bit less than 12% which proved previous study. The limnicity between terraces and distribution of lakes differs until several times, which can be explained by strong connection of hydrological and geomorphological factors.

Characteristic of limnicity, and lakes distribution is complicated due to different minimal reference areas of lakes, accepted for calculations. Comparison of results can't be direct because number of detected lakes and ponds depends on the spatial resolution of initial data. By far the most common type of water bodies in the study region is polygonal ponds.

According to Morgenstern (2008) the total area of lakes ≥ 20 ha is 1,861.8 km², or 6.4 % of the delta area, as the delta area assumed to be 29,000 km² (Schneider et al., 2009). Schnieder et al., (2009) relying on Landsat -7 imagery classification determined a surface covered by lakes with lakes area more than 0.36 ha – 3008 km², or 33.8% of the Lena River Delta land area. Boike et al., (2013) found that the limnicity of Samoilov island is about – 15%. Results of this study show that about 189,000 ponds and lakes cover a bit higher area in comparison with previous studies – about 3,390 km² or 11.7% of the entire Lena River Delta. In comparison with another Arctic deltas, for example the Mackenzie River Delta, where lakes occupy about 25% of entire delta (Walker, 1998), or the Kolyma Delta tundra zone where limnicity is found to be 13.5 % (Veremeeva and Glushkova, 2016), limnicity of the Lena River Delta isn't high.

Bolshiyanov et al., (2013) relying on the map 1:100 000 found 29,483 lakes (which is more than in 6 times less in comparison with our study), including 27165 lakes with an area under 0.25 km², 0.25 till 1 km² – 1817, from 1 km² till 5 km²– 443, from 5 till 10 km²– 48, 10 lakes with an area more than 10 km². Our study shows that the number of lakes with an area less than 0.25 km² is in almost in seven times higher. But in the other size classes was received slightly smaller numbers. Significant difference in the number of small lakes and ponds can be explained by difference in resolution of initial data. Differences in larger lakes can be explained by descent of lakes for the last 30 years. Obtained results also shows that the limnicity of Arga island is highest all over the delta, which correspond with data of lakes distribution presented with Bolshiyanov et al., (2013).

Mean lake area in the delta is about 18,000 m². This is under previous estimations (Morgenstern et al., 2008) due to difference in spatial resolution. Relatively great lakes, mean area is larger than 20,000 m² are situated mostly on the second terrace in the eastern part of the delta, probably due to antiquity of this part (Bolshiyanov et al., 2013).

According visual estimations majority of present thermokarst lakes in the depressions all over the delta are apparently smaller than the depressions, which was also marked by Grosse et al., (2005). Such inequality of area is most prominent on the Bykovsky peninsula and on the third terrace and caused by constant changes of thermokarst. Shrinking of taw lakes in the permafrost affected regions of northern Russia caused mainly by river drainage and vegetating (Kravtsova and Rodionova, 2016).

The Lena River Delta is generally lowland because the first terrace occupies the biggest area and this is displayed in the mean height of lakes level, which is only 5.9 m a.s.l. But differences in structure and origin of various parts of the delta are reflected in the broad heights distribution of water bodies elevation from 0 until 65 m a.s.l. and significant standard deviation of elevation series, more than 5 m. In light of the above it is difficult to compare the Lena River Delta with other arctic deltas like the Colville or the Mackenzie River deltas in sense of lakes sizes and elevation.

1st terrace

The first terrace is the youngest from main terraces in the Lena River Delta. An age of the central part of the terrace is about 8 thousand years and decreases towards

shore line until several hundreds of years (Bolshiyanov et al., 2013). Thus the structure of this terrace displays modern and Holocene fluvial dynamics.

Presented in this study section shows the significant difference in elevation between the central part and coastal parts of this terrace. Elevation of lakes shorelines levels in the central part are basically between 6 and 8 m a.s.l., in comparison with 0 – 2 m a.s.l. near to the shore of Laptev Sea. This coincides with data presented by Bolshiyanov et al., (2013): elevation of terrace in the middle part is about 10 - 12 m a.s.l., which falls on 10 -12 m towards the coastal margins. Such inequality in elevation of one terrace is caused by significant difference in the age of areas. The mean elevation of lake shorelines on this terrace is closer to elevation of margins, where frequency of water bodies id higher than in central part.

Morgenstern et al., (2008) found that there are 1,796 lakes with an area more than 20 ha, which cover 997 km² on the 1st terrace, and limnicity of terrace is 6.3% correspondingly. In this study was determined in 17 times more water objects, which cover an area more than in two times larger comparing to previous studies. Such considerable difference, relatively to this study, origins from taking into account not only thermokarst lakes but also ponds and polygonal lakes, which are frequent in this part of the delta.

Thus lakes on the first terrace are on average small with low elevation. This correlates well with genetic types of lakes typical for such environment: polygonal ponds and lakes, small circular thermokarst lakes and abandoned lakes. Abandoned lakes resulting from channel braiding and from meandering (oxbow lakes) are especially typical for this terrace, which is proved by the mode of elevation and concentration of heights of 75% of lakes near to sea level.

2nd terrace

The 2nd terrace is intermediate in the Lena River Delta by area and elevation, maximal heights of surface reach 30 m a.s.l. Elevation differences of surface is until 10 m (Bolshiyanov et al., 2013). The surface is characterized by thermokarst lakes, alases. Currently there are some difficulties in understanding of the genesis of large water bodies on the second terrace. It is only clear that the origin is connected with ice-wedges thaw (Bolshiyanov et al., 2013).

Limnicity especially of Island Arga, which is the main part of terrace, is highest (>17%) in the Lena River Delta. More than 52,000 lakes cover an area of 1,052 km². Mean elevation of lakes is about 10 m a.s.l., which also points on abundance of

thermokarst basins forming since early Holocene. Important feature of the second terrace is size of lakes. On this terrace large lakes predominate. This is caused by the conjunction of lakes through termoerosion valleys or union of lakes, but the lakes basins preserve the individuality through the deep central parts, which can be distinguished on satellite images or DEM.

3rd terrace

The 3rd terrace presented as individual islands formed from sandy sequences covered by "Ice Complex" is the smallest but the highest from the main geomorphological units in the Lena River Delta. An elevation of the relic terrace varies between 20 and 60 m a.s.l., and average value is about 35-40 m a.s.l. (Bolshiyanov et al., 2013). The terrace can be subdivided into two areas due to more than 20 m difference in altitude between the western and the eastern sector (Grigoriev, 1993). This difference is not so large but noticeable in the lakes elevation. Average elevation of lakes shorelines on this terrace is 20 m a.s.l. and it coincides with bottom estimation of terrace elevation. Moreover the distribution of lakes by elevation shows larger dispersion than other terraces. It can be caused by thermokarst lakes which have large weight among the lakes and are situated in thermokarst basins with various depths. The highest lakes all over the delta are situated in the centre of Kharadang Island with an elevation more than 60 m a.s.l.

Morgenstern (2012) detected 2,327 water bodies (minimum one pixel, 900 m²) with a total area of 88.3 km² considering 98.6% of the third terrace area (1,711.6 km²). Due to difference in resolution in our study were obtained much more lakes (4,010 ≥ 100 m²) with a total area of 97.86 km² which is 5.7% of a 3rd terrace area. It is obvious, that results coincide with each other considering absence of small ponds in the study of Morgenstern (2012).

Lakes coverage of 5.7% is the smallest among terraces in the Lena River Delta as well it is low compared to other arctic tundra regions like the western arctic coastal plain of Alaska with about 20 % lake coverage Morgenstern (2012).

The thermokarst basins mostly significantly exceed thermokarst lakes situated within them, which can be an evidence of recent lakes drainage on the 3rd terrace. Moderate changes of permafrost in the Lena River Delta for the last 30 years are connected with descend of small thermokarst lakes on the third terrace (Kravtsova and Bystrova, 2009). Generally characteristics of the lakes on the third main terrace are

typical for thermokarst lakes in ice-rich permafrost and controlled by the thermokarst process.

Bykovsky Peninsula study area

In our study was considered not only Bykovsky Peninsula but also adjacent lower part of Khorogor Valley. Bykovsky Peninsula is a Pleistocene accumulation plain. Therefore the relief of the peninsula is dominated by flat elevated areas up to 40 m a.s.l., maximum elevation is 43 m a.s.l. The area of the Bykovsky Peninsula occupied by lakes is less than the area occupied by thermokarst depressions according Grosse et al., (2005) in three times. This shows probable decreasing of lakes since the Late Pleistocene Holocene transition. A lot of modern lakes appeared during the Holocene in the old drained basins. The thermokarst depressions according to Grosse et al., (2007) mostly have steep slopes and very low mean elevations of 1–8 m a.s.l. and cover 46% of the entire area.

Grosse et al., (2008) calculated that lake cover by land area at BYK is 15.4%, or 2,053 ha are covered by 32 lakes with an area > 10 ha. In this study were detected 345 lakes with an area > 225 m², which cover 16.41 km², or 9.5% of BYK area. In the combined region of lower of Khorogor Valley and BYK Grosse et al., (2005) mapped 569 water bodies with an area > 186 m². Such number is compatible with results obtained in our study - 526 lakes, including only the neighbor to BYK part of Khorogor Valley.

Mean elevation of water bodies above 10 m a.s.l. can be explained due to combination of lakes situated on flat elevated areas, with maximal lakes height about 40 m a.s.l., and lakes situated in the deep thermokarst basins with lakes elevations less than 5 m a.s.l. up to 0 m a.s.l. For example, the largest lake on the BYK with an area about 6 km² situated in the vast thermokarst basin is elevated only on 0.5 m a.s.l. This difference is displayed in STD (Standard Deviation) of lakes elevation, which equals to 12.6 m, the highest dispersion among all studied areas.

5. Conclusions

This study is aimed at comprehensive mapping of the Lena Delta region water body and lake level height mapping based on remote sensing data and GIS methods. Ponds, polygonal and thermokarst lakes are a major component of vast arctic and subarctic landscapes in Siberia. Changes in the extent, number and elevation of these water objects, which are typical for permafrost affected territories, can be viewed as critical indicators of landscapes response to climate changes. Spatial altitudinal analysis of water features plays an important role in understanding thermokarst variability in polar region and impacts on the global hydrological and chemical cycles.

The Lena Delta is the largest arctic delta and its complicated structure, conditioned by the modern deltaic processes, presented in the first terrace, and various types of past dynamics reflected by the second and the third terrace correspondingly. Such diversity underlines the Lena Delta among other arctic deltas. Thus the Lena Delta and adjacent Bykovsky Peninsula is a crucial territory for studying of subarctic periglacial ecosystem changes, caused by permafrost variability foremost expressed in the thermokarst and thermal erosion.

Applied methodology, based on the Remote Sensing data, GIS handling and statistical calculations allows to map and to determine an elevation of water bodies with high accuracy. Using of two sets of high-resolution images acquired by two satellite surveying systems RapidEye and SENTINEL-2, was created two compositions of orthorectified and atmospherically corrected images, which jointly covers entire study region. Thus, taking into account previous study designated that in near and mid-infrared wavelengths water bodies are easily distinguishable from other land cover types, overlay of near-infrared bands of images was carried out at which each output cell value was set as a minimum value of the values assigned to the corresponding cells in the input images. For further extraction of water bodies was applied a common method of grey-level thresholding for mosaic separately. Comprehensive scheme of water bodies was created after filtering and refinement of overlay results. To determine elevation values of acquired lakes as initial data were used heights extracted from improved water mask of DEM TanDEM-X. Received results were checked and compared with laser altimetry data collected by ICESat observing mission. The comparison of two elevation sets showed minor discrepancies. Thus used in this study methodology shows its applicability for mapping and further analysis.

In addition during the execution of this thesis were carried out several practice investigations aimed at determination of the suitable methods of morphological filtering and refinement of DEM water mask.

As a result, 198851 water features with a size of more than 100 m² were mapped the first time in the region of the whole Lena Delta and adjacent Bykovsky Peninsula. For 189497 ponds and lakes that cover about 3426 km² were determined heights of water edge. Obtained spatial and elevation data fairly accurate display the division of the delta on three main terraces. Estimation of results shows a significant scattering of lakes characteristics and heights, as well as differences of limnicity between main geomorphological terraces. A mean elevation of lakes changes from 20 m a.s.l. for lakes situated on the 3rd terrace to 4.5 m a.s.l. for lakes on the first terrace. Profiles show general decline trend towards the eastern, modern margin of the delta. Thus data mentioned above correspond well with previous studies connected with analysis of lakes spatial features and distribution as well as terraces heights values assessment. However worth saying that using of high resolution data allowed us to newly estimate the number of small ponds and their influence on statistical features of water bodies in the region of interests, in comparison with previous studies.

Moreover this study opens a lot of opportunities for further continuation of research, especially connected with the determination of river channel inclination. This objective hasn't been achieved in presented work. It is planned in near feature to receive inclination of water channels, because main preparation steps, including a mapping of river channels for the whole delta have been already done.

6. Acknowledgements

I would like to express my gratitude to my supervisor from the German side Dr. Frank Günther for the continuous support of my master thesis and related research, for his patience, perfect knowledge in fields of remote sensing and permafrost. His guidance helped me in all the time of research and writing of my master thesis.

I would like to express my sincere gratitude to my supervisor from the Russian side Dr. Irina Fedorova for the remarks, helpful comments and his participating in the discussion of this master thesis.

My sincere thanks goes to The Alfred Wegener Institute (Potsdam) and PETA-CARB project team, especially to Prof. Dr. Guido Grosse. Without his immense support, it would not have been possible to conduct this study.

Furthermore, I would like to thank whole staff of Master Program for Polar and Marine Sciences (POMOR) in particular Dr. Nadezhda Kakhro, Dr. Heidemarie Kassens and Prof. Dr. Eva-Maria Pfeiffer for their permanent and comprehensive support.

7. References

Alekseevsky, N., 2007. Geoecological state of Russian Arctic coast and their safety of nature management, GEOS Publ.,Moscow, Russia, 586 p (in Russian).

AMAP, 2011. Snow, Water, Ice and Permafrost in the Arctic (SWIPA): Climate Change and the Cryosphere.

Antonova S., Duguay Claude R; Kääb A.; Heim B.; Langer M.; Westermann S.; Boike J., 2016. Monitoring bedfast ice and ice phenology in lakes of the Lena River Delta using TerraSAR-X backscatter and coherence time series. Remote Sensing, 8(11): 903.

Aret F., Reimnitz E., 2000. An Overview of the Lena River Delta Setting: Geology, Tectonics, Geomorphology and Hydrology. Journal of Coastal Research, Vol. 16, 4: 1083-1093.

Behling, R., Roessner, S., Kaufmann, H. & Kleinschmit, B., 2014. Automated Spatiotemporal Landslide Mapping over Large Areas Using RapidEye Time Series Data. Remote Sensing, 6: 8026-8055.

Bernardo N., Watanabe F., Rodrigues T., Alcantara E., 2017. Atmospheric correction issues for retrieving total suspended matter concentrations in inland waters using OLI/Landsat-8 image Advances in Space Research Volume 59, Issue 9: 2335–2348.

Boike, J., Wille, C., Abnizova, A., 2008. Climatology and summer energy and water balance of polygonal tundra in the Lena River Delta, Siberia Journal of Geophysical Research: 113.

Boike, J., Kattenstroth, B., Abramova, K., Bornemann, N., Chetverova, A., Fedorova, I., Fröb, K., Grigoriev, M., Grüber, M., Kutzbach, L., Langer, M., Minke, M., Muster, S., Piel, K., Pfeiffer, E.-M., Stoof, G., Westermann, S., Wischnewski, K., Wille, C., and Hubberten, H.-W., 2013. Baseline characteristics of climate, permafrost and land cover from a new permafrost observatory in the Lena River Delta, Siberia (1998–2011), Biogeosciences, 10: 2105–2128.

Bolshiyanov, D., Makarov, A., Schneider V. and Stof G., 2013. Evolution and development of the Lena River delta, Publ. of AARI, St. Petersburg, Russia, 268 p (in Russian).

Drachev, S. S., Savostin, L. A., Groshev, V. G., Bruni, I. E., 1998. Structure and geology of the continental shelf of the Laptev Sea. Eastern Russian Arctic Tectonophysics, 298: 357 – 393.

Grigoriev, N.F., 1960. The temperature of permafrost in the Lena Delta basin: Deposit conditions and properties of the permafrost in Yakutia, 2: 97–101 (in Russian).

Grigoriev, M.N., 1993. Criomorphogenesis in the Lena Delta. Permafrost Institute Press, Yakutsk, 176 (in Russian).

Grigoriev, M., Rachold, V., Schirrmeister, L., Hubberten, H.-W. Stein, R., Macdonald, R., 2004. The organic carbon cycle in the Arctic Ocean: present and past, Springer. Berlin, 37-65.

Grosse, G., Schirrmeister, L., Kunitsky, V.V., Hubberten, H.-W., 2005.The use of CORONA images in remote sensing of periglacial geomorphology: an illustration from the NE Siberian coast. Permafrost and Periglacial Processes 16: 163–172.

Grosse, G., Romanovsky, V., Walter, K., Morgenstern, A., Lantuit, H., Zimov, S., 2008. Distribution of thermokarst lakes and ponds at three Yedoma sites in Siberia. Proceedings of the 9th International Conference on Permafrost, Fairbanks, Alaska, 29 June - 3 July 2008, Kane, D. L. and Hinkel, K. M. (Eds.), Institute of Northern Engineering, University of Alaska Fairbanks: 551-556.

Grosse, G.; Romanovsky, V.; Jorgenson, T.; Walter Anthony, K.; Brown, J. & Overduin, P., 2011. Vulnerability and feedbacks of permafrost to climate change Eos Trans. AGU, AGU, 92: 73-74.

Grosse G., Jones B., and Arp C., 2013. Thermokarst Lakes, Drainage, and Drained Basins. In: John F. Shroder (Editor-inchief), Giardino, R., and Harbor, J. (Volume Editors). Treatise on Geomorphology, Vol 8, Glacial and Periglacial Geomorphology, San Diego: Academic Press: 325-353

Günther, F., Overduin, P. P., Sandakov, A. V., Grosse, G., Grigoriev, M. N., 2013. Short- and long-term thermo-erosion of ice-rich permafrost coasts in the Laptev Sea region. Biogeosciences, 10: 4297-4318.

Günther, F., Overduin, P. P., Yakshina, I. A., Opel, T., Baranskaya, A. V. & Grigoriev, M. N., 2015. Observing Muostakh disappear: permafrost thaw subsidence and erosion of a ground-ice-rich island in response to arctic summer warming and sea ice reduction. The Cryosphere, 9: 151-178.

Jorgenson, M. T., and Grosse, G., 2016. Remote Sensing of Landscape Change in Permafrost Regions. Permafrost and Periglacial Processes, 27: 324–338.

Kravtsova, V. I., Bystrova, A. G., 2009. Changes in thermokarst lake sizes in different regions of Russia for the last 30 years. Kriosfera Zemli (Earth Cryosphere) 13: 16-26. (in Russian).

Kravtsova, V. I., Tarasenko, T. V., 2011. The dynamics of thermokarst lakes under climate changes since 1950, Central Yakutia. Kriosphera Zemli (Earth Cryosphere) 15 (3): 31-42. (in Russian).

Kravtsova, V. I., Rodionova, T.V., 2016. Variations in size and number of thermokarst lakes in different permafrost regions: spaceborne evidence. Kriosfera Zemli (Earth Cryosphere) 20: 75-81.

Kokelj, S. V. and Jorgenson, M. T., 2013. Advances in Thermokarst Research. Permafrost and Periglac. Process., 24: 108–119.

Kuhry, P., Grosse, G., Harden, J. W., Hugelius, G., Koven, C. D., Ping, C.-L., Schirrmeister, L. and Tarnocai, C., 2013. Characterisation of the Permafrost Carbon Pool. Permafrost and Periglac. Process., 24: 146–155.

Morgenstern, A., Grosse, G., Schirrmeister, L., 2008. Genetic, morphological, and statistical characterization of lakes in the permafrost-dominated Lena Delta, in: Proceedings of the 9th International Conference on Permafrost, Fairbanks, Alaska, 29 June - 3 July 2008, Kane, D. L. and Hinkel, K. M. (Eds.), Institute of Northern Engineering, University of Alaska Fairbanks: 1239-1244.

Morgenstern A.,Grosse G., Gunther F., Fedorova I., and Schirrmeister L., 2011 Spatial analyses of thermokarst lakes and basins in Yedoma landscapes of the Lena Delta. The Cryosphere Discuss., 5: 1495–1545.

Morgenstern, A., 2012 .Thermokarst and thermal erosion: Degradation of Siberian ice-rich permafrost. PhD thesis, Univ.Potsdam, 116 p.

Morgenstern A., Ulrich M., Günther F., Roessler S., Fedorova I., Rudaya N., Wetterich S., Boike J., Schirrmeister L., 2013. Evolution of thermokarst in East Siberian ice-rich permafrost: A case study. Geomorphology, 201: 363–379.

Muster S., Langer M., Heim B., Westermann S., Boike J., 2012. Subpixel heterogeneity of ice-wedge polygonal tundra: a multi-scale analysis of land cover and evapotranspiration in the Lena River Delta, Siberia. Tellus B, 64.

Muster, S., Heim, B., Abnizova, A., Boike, J., 2013. Water Body Distributions Across Scales: A Remote Sensing Based Comparison of Three Arctic Tundra Wetlands. Remote Sensing, 5: 1498-1523.

Nitze I., Grosse G., 2016. Detection of landscape dynamics in the Arctic Lena Delta with temporally dense Landsat time-series stacks Remote Sens. Environ., 181: 27–41.

PCI, 2015: ATCOR- Ground Reflectance Workflow Geomatica 2015 Tutorial, 11 p.

Proshutinsky, A., Ashik, I., Dvorkin, E., Häkkinen, S., Krishfield, R., Peltier, W., 2004. Secular sea level change in the Russian sector of the Arctic Ocean. Journal of Geophysical Research: Oceans: 109.

Rachold, V., Grigoriev, M.; Are, F.; Solomon, S.; Reimnitz, E.; Kassens, H. & Antonow, M., 2000. Coastal erosion vs riverine sediment discharge in the Arctic Shelf seas, International Journal of Earth Sciences, Springer-Verlag, 89: 450-460.

Schneider J., Grosse G., Wagner D., 2009. Detection of landscape dynamics in the Arctic Lena Delta with temporally dense Landsat time-series stacks. Remote Sensing of Environment 113: 380–391.

Schwamborn, G., Rachold, V., Grigoriev, M., 2002. Late Quaternary sedimentation history of the Lena Delta Quaternary International, 89: 119-134.

Schirrmeister, L., Grosse, G., Schwamborn, G., Andreev, A., Meyer, H., Kunitzky, V., Kuznetsova, T., Dorozhkina, M., Pavlova, E., Bobrov, A., Oezen, D., 2003. Late Quarternary history of the accumulation plain north of the Chekanovsky Ridge (Lena Delta, Russia). A multidisciplinary approach Polar Geography, 27: 277-319.

Schirrmeister, L., Grosse, G., Schnelle, M., Fuchs, M., Krbetschek, M., Ulrich, M., Kunitsky, V., Grigoriev, M., Andreev, A., Kienast, F., Meyer, H., Babiy, O., Klimova, I., Bobrov, A., Wetterich, S., Schwamborn, G., 2011. Late Quaternary paleoenvironmental records from the western Lena Delta, Arctic Siberia Palaeogeography, Palaeoclimatology, Palaeoecology, 299: 175-196.

SENTINEL-2 User handbook, 2015: ESA Standard Document, Issue 1 Rev 2, 64p.

TanDEM-X, 2016: Ground Segment DEM Products Specification Document, issue 3.1, EOC – Earth Observation Center, 46 p.

Ulrich, M., Grosse, G., Chabrillat, S. and Schirrmeister, L., 2009. Spectral characterization of periglacial surfaces and geomorphological units in the Arctic Lena Delta using field spectrometry and remote sensing. Remote Sensing of Environment, 113: 1220-1235.

van Everdingen, R. O. (Ed.), 2005. Multi-language glossary of permafrost and related groundice terms, National Snow and Ice Data Center/World Data Center for Glaciology, Boulder. Available at: http://nsidc.org/fgdc/glossary.

Vaudoura E., Gilliota J.M., Belc L., Bréchetb L., Hamiachec J., Hadjarb D., Lemonnierb Y., 2014. Uncertainty of soil reflectance retrieval from SPOT and RapidEye multispectral satellite images using a per-pixel bootstrapped empirical

line atmospheric correction over an agricultural region. International Journal of Applied Earth Observation and Geoinformation, 26: 217–234.

Veremeeva, A.A., Glushkova N.V., 2016. Formation of relief in the regions of ice complex deposits distribution: remote sensing and GIS studies in the Kolyma lowland tundra. Kriosfera Zemli (Earth Cryosphere), 20 (1): 14–24

Walker, H.J. 1998. Arctic deltas. Journal of Coastal Research 14: 718-738.

Zhang T., Barry R.G., Knowles K., Heginbottom J.A., Brown J., 2008. Statistics and characteristics of permafrost and ground-ice distribution in the Northern Hemisphere. Polar Geogr., 31: 47–68.

Zubrzycki, S.; Kutzbach, L.; Grosse, G.; Desyatkin, A. , Pfeiffer, E.-M., 2013. Organic carbon and total nitrogen stocks in soils of the Lena River Delta, Biogeosciences, 10: 3507-3524.

Internet sources:

Awi.de, 2016. Alfred Wegener Institute PETA-CARB. [online] Available at: https://www.awi.de/en/science/junior-groups/peta-carb

GRASS GIS 7.3.svn, 2017 Reference Manual. [online] Available at: https://grass.osgeo.org/grass73/manuals/r.series.

eoportal.org, 2017 [online] Available at: https://directory.eoportal.org/web/eoportal/satellite-missions/r/rapideye.

gis-lab.info, 2017. Orthocorrection of space images using RPC. [online] Available at: http://gis-lab.info/qa/ortho-rpc.html.

GRASS GIS 7.3.svn, 2017. Reference Manual. [online] Available at: https://grass.osgeo.org/grass73/manuals/r.series.

dst-iget.in, 2017 Introduction to SAGA. [online] Available at: http://dst-iget.in/tutorials/iget-rs/iget-rs-001

Statement on the thesis' originality

Herewith I, Aleksandr Volynetc, declare that I wrote the thesis independently and did not use any other resources than those named in the bibliography, and, in particular, did not use any Internet resources except for those named in the bibliography. The master thesis has not been used previously as part of an examination. The master thesis has not been previously published.